

Color superconductivity in weak coupling

Robert D. Pisarski*

*Department of Physics, Brookhaven National Laboratory, Upton, New York 11973*Dirk H. Rischke[†]*RIKEN-BNL Research Center, Brookhaven National Laboratory, Upton, New York 11973*

(Received 21 October 1999; published 6 March 2000)

We derive perturbatively the gap equations for a color-superconducting condensate with total spin $J=0$ in dense QCD. At zero temperature, we confirm the results of Son for the dependence of the condensate on the coupling constant, and compute the prefactor to leading logarithmic accuracy. At nonzero temperature, we find that to leading order in weak coupling, the temperature dependence of the condensate is identical to that in BCS-like theories. The condensates for total spin $J=1$ are classified; to leading logarithmic accuracy these condensates are of the same order as those of spin $J=0$.

PACS number(s): 12.38.Mh, 24.85.+p

I. INTRODUCTION

Cooper's theorem [1–3] implies that if there is an attractive interaction in a cold Fermi sea, the system is unstable with respect to the formation of a particle-particle condensate. In QCD, single-gluon exchange between quarks of different color generates an attractive interaction in the color-antitriplet channel [4]. Thus, it appears unavoidable that color superconductivity occurs in dense quark matter which is sufficiently cold [5–20]. How a dense quark phase matches onto hadronic matter is difficult to address [7,11]. In particular, while a quark-quark condensate may form, such condensation competes with the tendency of a quark-quark pair to bind with a third quark, to form a color-singlet hadron.

One way of understanding color superconductivity is to compute at very high densities, where by asymptotic freedom, perturbation theory can be used. At nonzero temperature, but zero quark density, it is well known that perturbation theory is a particularly bad approximation [21]. If g is the coupling constant for QCD, the free energy is not an expansion in g^2 , but only in g , with a series which is well behaved only for $g \leq 1$. In contrast, at zero temperature and nonzero quark density, the free energy is an expansion in $g^2 \ln(1/g)$, and appears to be well behaved for much larger values of the coupling constant, up to values of $g \leq 4$ [22]. Similar conclusions can be reached by comparing the gluon ‘‘mass,’’ $m_g \sim g\mu$ or $\sim gT$, to the chemical potential, μ , or the temperature, T [15]. Thus for cold, dense quark matter, perturbation theory might give us information which not even lattice QCD calculations can provide.

Color superconductivity is rather different from ordinary superconductivity, as in the model of Bardeen, Cooper, and Schrieffer (BCS) [1–3]. In BCS-like theories, superconductivity is determined by infrared divergences which arise in the scattering between two fermions close to the Fermi surface: the initial fermions, with momenta \mathbf{k} and $-\mathbf{k}$, scatter into a pair with momenta \mathbf{k}' and $-\mathbf{k}'$. Summing up bubble

diagrams generates an instability which is only cured by a fermion-fermion condensate. If the fermions interact through a point-like four-fermion coupling, though, there is no correlation between the initial and outgoing momenta, \mathbf{k} and \mathbf{k}' . In the gap equation, this implies that the gap function is constant with respect to momentum, as long as the momenta are near the Fermi surface.

In QCD, however, scattering through single-gluon exchange strongly correlates the direction of the in- and outgoing quarks: there is a logarithmic divergence for forward-angle scattering, $\sim \int d\theta/\theta$. This extra logarithm from forward scattering implies that the gap is not an exponential in $1/g^2$, as in BCS-like theories, but only in $1/g$ [7,8,13,15]. As a consequence, the gap function is no longer constant as a function of momentum, even about the Fermi surface.

The logarithmic divergence for forward-angle scattering arises because in cold, dense quark matter, static, magnetic interactions are not screened through a ‘‘magnetic mass.’’ This is very different from a system of hot quarks and gluons. Over large distances, a hot system is essentially three dimensional; gluons in three dimensions have powerlike infrared divergences, which screen static, magnetic fluctuations through a magnetic mass $\sim g^2 T$. In contrast, loop corrections in cold, dense quark matter are essentially four dimensional; infrared divergences are at worst logarithmic, so that any magnetic mass is at best $\sim \mu \exp(-1/g^2)$, which is much smaller than the scale for color superconductivity, $\sim \mu \exp(-1/g)$ [7,8].

The dependence of the zero-temperature color-superconducting spin-zero condensate ϕ_0 on the QCD coupling constant g was first computed by Son [8], who used a beautiful renormalization-group analysis to show that

$$\phi_0 = 2 \frac{b_0}{g^5} \mu \exp\left(-\frac{\pi}{2g}\right). \quad (1)$$

Here $\bar{g} = g/(3\sqrt{2}\pi)$ arises naturally from the solution, assuming three colors. In Son's result, $2b_0$ is a pure number of order 1.

In this paper we derive the gap equations for a condensate with total spin $J=0$ and $N_f=2$ massless quark flavors, at an

*Email address: pisarski@bnl.gov

[†]Email address: rischke@bnl.gov

arbitrary temperature T . Our derivation is perturbative, i.e., $g \ll 1$. In this case there are three scales in cold, dense QCD, the chemical potential μ , the gluon mass $m_g \sim g\mu$, and the color-superconducting condensate $\phi_0 \sim \mu \exp(-1/g)$, and they are naturally ordered, $\mu \gg m_g \gg \phi_0$.

We solve the gap equations to ‘‘leading logarithmic accuracy,’’ by which we mean the following. In the gap equations, the leading terms are $\sim \ln(\mu/\phi_0)$. These terms generate the exponential in $1/g$ in Eq. (1); therefore $\ln(\mu/\phi_0)$ is of order $1/g$. There are also leading logarithmic terms $\sim \ln(\mu/m_g)$, which are $\sim \ln(1/g)$ plus a constant. The $\ln(1/g)$ gives rise to the prefactor $1/g^5$, while the constant contributes to b_0 . For N_f flavors of massless quarks we find

$$b_0 = 256 \pi^4 \left(\frac{2}{N_f} \right)^{5/2} b'_0. \quad (2)$$

There are other terms in the gap equations, which do not arise from $\ln(\mu/m_g)$. These terms are of order 1, and thus of the same order as the constant term originating from the logarithm $\ln(\mu/m_g)$. Hence they contribute in the same way to b_0 . We do not compute these, so that in Eq. (2) there is an undetermined constant b'_0 .

Our results were described previously [15], and agree completely with an independent analysis by Schäfer and Wilczek [13]; they also overlap with those of Hong *et al.* [12]. The factor $N_f^{-5/2}$ in Eq. (2) originates from the N_f dependence of m_g ; however, b'_0 will also depend on N_f [19].

Even though we do not determine b'_0 , it is very interesting that the numerical value of b_0/b'_0 is large. This implies that, for chemical potentials of order ~ 1 GeV, the gap can be of order 100 MeV [13,15]. Such large values of the gap are in accord with previous estimates obtained within Nambu–Jona-Lasinio models [5], and are much larger than original estimates by Bailin and Love, $\phi_0 \sim 1$ MeV [4].

We then solve the gap equations at nonzero temperature. We find a surprising result: while the detailed form of the gap function is very different in QCD versus BCS-like theories, the temperature dependence of the condensate—the dimensionless ratio of the condensate at a temperature T to that at zero temperature, $\phi(T)/\phi_0$ —is *identical* to BCS-type theories. In particular, the ratio of the critical temperature, $T_c/\phi_0 \approx 0.567$, is as in BCS [1,2]. Our result for $\phi(T)/\phi_0$ is valid to leading order in weak coupling, even though we cannot compute the overall magnitude of ϕ_0 , i.e., b'_0 . In our mean-field approximation the transition is of second order, but the transition can be driven first order by critical fluctuations near the would-be critical point [7].

We then classify the condensates with total spin $J=1$. Following our classification of condensates with $J=0$, which employed projectors for chirality, helicity, and energy, we show that there are two types of spin-1 condensates, longitudinal and transverse. As an example, we solve the gap equations for $N_f=1$ and find

$$\phi_1 = 2 \frac{b_1}{g^5} \mu \exp\left(-\frac{\pi}{2g}\right), \quad b_1 \equiv \frac{b_0}{b'_0} b'_1. \quad (3)$$

That is, not only is the parametric dependence of the spin-1 condensates on g the same as for spin 0, as argued originally by Son [8], but to leading logarithmic accuracy, even the constant in front is the same. We do not expect that b'_1 , the undetermined constant analogous to b'_0 , is the same. Surely b'_1 is smaller than b'_0 , and depends on whether the condensate is longitudinal or transverse. This is very different from BCS-like theories, where condensates with higher spin are typically exponentially suppressed. In QCD, higher-spin condensates are only suppressed by a pure number.

Nevertheless, one dramatic implication of our results is that superconductivity in QCD may be very unlike one’s intuition from nonrelativistic systems. Instead of higher-spin gaps being much smaller, they may be relatively large, which is important for phenomenology. Consider, for instance, a quark star with u , d , and s quarks. In the limit of high densities, when the strange quark mass m_s is negligible, the number of u , d , and s quarks are equal. Then charge neutrality is automatic, and the preferred color-superconducting condensates are of spin $J=0$, with color-flavor locking [6]. For realistic densities, however, the chemical potentials for u , d , and s will not be equal. The strange quark chemical potential differs from the up and down quark chemical potentials due to $m_s \gg m_u, m_d$. The up and down quark chemical potentials differ on account of charge neutrality. These effects suppress the color-antitriplet $J=0$ condensates, because they are composed of quarks with different flavor. On the other hand, the color-antitriplet $J=1$ condensates may form between quarks of the same flavor, and are not suppressed if the chemical potentials of the various flavors differ.

This paper is organized as follows. In Sec. II, we derive the gap equations for a spin $J=0$ condensate of $N_f=2$ massless flavors at an arbitrary temperature T . In Sec. III we solve these equations to leading logarithmic accuracy, first at $T=0$, and then at nonzero T . In Sec. IV we classify the possible spin $J=1$ condensates, and solve the gap equations for $N_f=1$. Section V concludes this work with a discussion of higher-order effects which contribute to b'_0 and b'_1 . Our units are $\hbar=c=1$; the metric tensor is $g^{\mu\nu} = \text{diag}(+, -, -, -)$. Four-vectors are denoted by capital letters, $K \equiv K^\mu = (k^0, \mathbf{k})$, and $k \equiv |\mathbf{k}|$, while $\mathbf{k} \equiv \mathbf{k}/k$.

II. GAP EQUATIONS

In general, a color-superconducting condensate $\Phi_{ij,fg}^+$ is a $N_c \times N_c$ matrix in fundamental color space ($i, j=1, \dots, N_c$), a $N_f \times N_f$ matrix in flavor space ($f, g=1, \dots, N_f$), and a 4×4 matrix in Dirac space [7]. As shown in [7], for $N_f=2$ a color-antitriplet condensate is a flavor singlet,

$$\Phi_{ij,fg}^+ \equiv \epsilon_{fg} \Phi_{ij}^+ \equiv \epsilon_{fg} \epsilon_{ijk} \Phi_k^+. \quad (4)$$

By a global color rotation, we can always choose Φ_k^+ to point in the 3-direction in color space, $\Phi_k^+ \equiv \delta_{k3} \Phi^+$. For $N_f=3$, even if we assume that the dominant condensate is a color antitriplet, there is always a small admixture of a color sextet [16]. The color-antitriplet condensate is a flavor anti-

triplet, and the color sextet a flavor sextet [7,19]. In this paper, for simplicity we consider only the case $N_f=2$.

The gap equation for a color-superconducting condensate of massless fermions was derived in [9] [cf. Eq. (A35) of [9]]. At a nonzero temperature T , this equation reads (we suppress fundamental color and flavor indices for the moment)

$$\begin{aligned} \Phi^+(K) &= g^2 \frac{T}{V} \sum_Q \bar{\Gamma}_a^\mu \Delta_{\mu\nu}^{ab}(K-Q) \\ &\times G_0^-(Q) \Phi^+(Q) G^+(Q) \Gamma_b^\nu. \end{aligned} \quad (5)$$

Here, $T/V \sum_Q \equiv T \sum_n \int d^3\mathbf{q} / (2\pi)^3$ in the infinite-volume limit [n labels the Matsubara frequencies $\omega_n \equiv (2n+1)\pi T \equiv iq_0$], and a summation over Lorentz indices μ, ν as well as adjoint color indices $a, b = 1, \dots, N_c^2 - 1$ is implied; $N_c = 3$ is the number of colors. $\Delta_{\mu\nu}^{ab}$ is the gluon propagator,

$$G_0^\pm(Q) \equiv (\gamma \cdot Q \pm \mu \gamma_0)^{-1} \quad (6)$$

is the propagator for *free*, massless particles (upper sign) or charge-conjugate particles (lower sign),

$$G^\pm \equiv \{[G_0^\pm]^{-1} - \Sigma^\pm\}^{-1} \quad (7)$$

is the propagator for *quasiparticles* (upper sign) or charge-conjugate quasiparticles (lower sign), and

$$\Sigma^\pm \equiv \Phi^\mp G_0^\mp \Phi^\pm \quad (8)$$

their self-energy arising from the interaction with the condensate. The charge-conjugate condensate is

$$\Phi^- \equiv \gamma_0 (\Phi^+)^\dagger \gamma_0, \quad (9)$$

and the vertices are

$$\Gamma_a^\mu \equiv T_a \gamma^\mu, \quad \bar{\Gamma}_a^\mu \equiv C (\Gamma_a^\mu)^T C^{-1} \equiv -\gamma^\mu T_a^T, \quad (10)$$

where γ^μ are the Dirac matrices and T_a the Gell-Mann matrices, $C = -C^\dagger = -C^T = -C^{-1} = i\gamma^2 \gamma_0$ is the charge conjugation matrix.

In the following, we analyze the flavor, color, and Dirac structure of the gap equation (5). For $N_f=2$, the color-flavor structure of the condensate (4) does not mix color and flavor indices, and thus the analysis of flavor and color can be done separately. This is different for $N_f=3$, where color rotations are locked to flavor rotations.

A. Flavor structure

We first discuss the flavor structure of Eq. (5). Fundamental color indices will be suppressed for the moment. The free propagator (6) is diagonal in flavor,

$$G_{0fg}^\pm(Q) \equiv \delta_{fg} G_0^\pm(Q) \equiv \delta_{fg} (\gamma \cdot Q \pm \mu \gamma_0)^{-1}, \quad (11)$$

and so is the self-energy,

$$\begin{aligned} \Sigma_{fg}^+ &= \gamma_0 (\Phi^+)_{fh}^\dagger \gamma_0 G_{0hi}^- \Phi_{ig}^+ = \epsilon_{hif} \delta_{hi} \epsilon_{ig} \gamma_0 (\Phi^+)^\dagger \gamma_0 G_0^- \Phi^+ \\ &= \delta_{fg} \gamma_0 (\Phi^+)^\dagger \gamma_0 G_0^- \Phi^+ \equiv \delta_{fg} \Sigma^+, \end{aligned} \quad (12)$$

and thus $G_{fg}^+ = \delta_{fg} G^+$. Therefore, both the left- and right-hand sides of Eq. (5) are simply proportional to ϵ_{fg} : the flavor structure of the gap equation is trivial in QCD with $N_f=2$ flavors, and will thus not be explicitly denoted in the following.

B. Color structure

The free propagator (6) is diagonal in the color indices for the fundamental representation,

$$G_{0ij}^\pm(Q) \equiv \delta_{ij} G_0^\pm(Q) \equiv \delta_{ij} (\gamma \cdot Q \pm \mu \gamma_0)^{-1}. \quad (13)$$

The self-energy Σ_{ij}^+ is also diagonal, but not all diagonal elements are equal:

$$\begin{aligned} \Sigma_{ij}^+ &= \gamma_0 (\Phi^+)_{ik}^\dagger \gamma_0 G_{0kl}^- \Phi_{lj}^+ = \epsilon_{ki3} \delta_{kl} \epsilon_{lj3} \gamma_0 (\Phi^+)^\dagger \gamma_0 G_0^- \Phi^+ \\ &\equiv (\delta_{ij} - \delta_{i3} \delta_{j3}) \Sigma^+, \end{aligned} \quad (14)$$

the self-energy for quarks with color 3 vanishes. This is easy to understand. Let us first note that, according to Eq. (A17) of [9], the condensate Φ^+ is actually proportional to $\langle \psi_C \bar{\psi} \rangle$, while $\Phi^- \sim \langle \psi \bar{\psi}_C \rangle$. ($\psi_C \equiv C \bar{\psi}^T$ is the charge-conjugate fermion field.) Thus, according to Eq. (8), the self-energy Σ^+ arises from the following process: a quark with, let us say, color 1 annihilates with a corresponding antiquark in Φ^+ , creating a charge-conjugate quark with color 2. This quark is propagated with the charge-conjugate propagator G_0^- , and annihilates with a charge-conjugate antiquark of color 2 in Φ^- , whereby a quark with color 1 is emitted. As only quarks with colors 1 and 2 condense, it is not possible to annihilate and create quarks with color 3 in this process; thus the latter do not attain a self-energy.

One can now compute the color structure of the quasiparticle propagator,

$$\begin{aligned} G_{ij}^+ &= \{ \delta_{ij} [G_0^+]^{-1} - (\delta_{ij} - \delta_{i3} \delta_{j3}) \Sigma^+ \}^{-1} \\ &= (\delta_{ij} - \delta_{i3} \delta_{j3}) G^+ + \delta_{i3} \delta_{j3} G_0^+, \end{aligned} \quad (15)$$

where $G^+ \equiv \{[G_0^+]^{-1} - \Sigma^+\}^{-1}$.

When inserted into the gap equation (5), the terms $\sim \delta_{i3} \delta_{j3}$ in Eq. (15) vanish, as $\Phi_{ij}^+ \sim \epsilon_{ij3}$. The gap equation becomes

$$\begin{aligned} \epsilon_{ij3} \Phi^+(K) &= -(T_{1i}^a T_{2j}^b - T_{2i}^a T_{1j}^b) g^2 \frac{T}{V} \sum_Q \gamma^\mu \Delta_{\mu\nu}^{ab}(K-Q) \\ &\times G_0^-(Q) \Phi^+(Q) G^+(Q) \gamma^\nu. \end{aligned} \quad (16)$$

From the explicit form of the Gell-Mann matrices we now infer that only gluons with adjoint colors 1, 2, 3, and 8 participate in the gap equation.

A color-superconducting condensate $\Phi_k^+ \sim \delta_{k3}$ breaks $SU(3)_c$ to $SU(2)_c$; gluons 1, 2, and 3 then correspond to the generators of the unbroken subgroup, and thus remain mass-

less, while the 8th gluon attains a mass through the Anderson-Higgs effect. Denoting $\Delta_{\mu\nu}^{11} = \Delta_{\mu\nu}^{22} = \Delta_{\mu\nu}^{33} \equiv \Delta_{\mu\nu}$ and $\Delta_{\mu\nu}^{88} \equiv \tilde{\Delta}_{\mu\nu}$, we obtain

$$\Phi^+(K) = \frac{3}{4} g^2 \frac{T}{V} \sum_Q \gamma^\mu \left[\Delta_{\mu\nu}(K-Q) - \frac{1}{9} \tilde{\Delta}_{\mu\nu}(K-Q) \right] \times G_0^-(Q) \Phi^+(Q) G^+(Q) \gamma^\nu, \quad (17)$$

where a common factor ϵ_{ij3} has been dropped from both sides of the gap equation.

In a complete treatment of the gap equations the effect of the condensate on the gluon propagator has to be included [20]. In contrast, we use the gluon propagator in the ‘‘hard dense loop’’ (HDL) approximation [23–26]. The HDL propagator introduces a gluon mass $m_g \sim g\mu$. Since in perturbation theory the scale of the condensate ϕ_0 is much smaller than m_g , it is reasonable to expect that, to a first approximation, we can neglect the effects of the condensate on the gluon propagator. A more detailed explanation is given below. We consequently assume $\tilde{\Delta}_{\mu\nu} \equiv \Delta_{\mu\nu}$, and obtain

$$\Phi^+(K) = \frac{2}{3} g^2 \frac{T}{V} \sum_Q \gamma^\mu \Delta_{\mu\nu}(K-Q) \times G_0^-(Q) \Phi^+(Q) G^+(Q) \gamma^\nu. \quad (18)$$

C. Dirac structure

In [9] we have shown that the gap matrix Φ^+ for a condensate with total spin $J=0$ has the form

$$J=0: \quad \Phi^+(K) = \sum_{h=r,\ell} \sum_{s=\pm} \sum_{e=\pm} \phi_{hs}^e(K) \mathcal{P}_{hs}^e(\mathbf{k}). \quad (19)$$

The 4×4 matrices $\mathcal{P}_{hs}^e(\mathbf{k})$ are defined as

$$\mathcal{P}_{hs}^e(\mathbf{k}) \equiv \mathcal{P}_h \mathcal{P}_s(\mathbf{k}) \Lambda^e(\mathbf{k}), \quad (20)$$

where \mathcal{P}_h are projectors for chirality, $h=r,\ell$,

$$\mathcal{P}_r = \frac{1+\gamma_5}{2}, \quad \mathcal{P}_\ell = \frac{1-\gamma_5}{2}, \quad (21)$$

while

$$\mathcal{P}_s(\mathbf{k}) = \frac{1+s\gamma_5\gamma_0\boldsymbol{\gamma}\cdot\hat{\mathbf{k}}}{2}, \quad s=\pm, \quad (22)$$

are projectors for helicity, and

$$\Lambda^e(\mathbf{k}) = \frac{1+e(\beta_{\mathbf{k}}\gamma_0\boldsymbol{\gamma}\cdot\hat{\mathbf{k}}+\alpha_{\mathbf{k}}\gamma_0)}{2}, \quad e=\pm, \quad (23)$$

are projectors for energy, $\beta_{\mathbf{k}} \equiv k/E_{\mathbf{k}}$, $\alpha_{\mathbf{k}} \equiv m/E_{\mathbf{k}}$, $E_{\mathbf{k}} \equiv \sqrt{k^2+m^2}$. While the $\mathcal{P}_{hs}^e(\mathbf{k})$ are composed of projectors, they are not projectors themselves [cf. Eq. (B29) in [9]], and thus were termed ‘‘quasiprojectors’’ in [9].

In the ultrarelativistic limit, $m=0$, the energy projectors simplify to

$$m=0: \quad \Lambda^e(\mathbf{k}) = \frac{1+e\gamma_0\boldsymbol{\gamma}\cdot\hat{\mathbf{k}}}{2}. \quad (24)$$

This has three major consequences. First, the quasiprojectors (20) become true projectors [cf. Eq. (B29) of [9]]. Second, $\mathcal{P}_{r+} = \mathcal{P}_{r-} = \mathcal{P}_{\ell+} = \mathcal{P}_{\ell-} \equiv 0$, expressing the fact that right-handed, positive-helicity particles cannot have negative energy, etc. [cf. Eq. (B30) of [9]]. Third, *either* the chirality, *or* the helicity, *or* the energy projector in Eq. (20) becomes superfluous [cf. Eq. (B31) of [9]]. In the following, we omit the helicity projector and use just chirality and energy projectors,

$$m=0: \quad \mathcal{P}_{hs}^e(\mathbf{k}) \rightarrow \mathcal{P}_h^e(\mathbf{k}) \equiv \mathcal{P}_h \Lambda^e(\mathbf{k}). \quad (25)$$

Then, Eq. (19) simplifies to [cf. Eq. (8) of [9]]

$$J=0, m=0: \quad \Phi^+(K) = \sum_{h=r,\ell} \sum_{e=\pm} \phi_h^e(K) \mathcal{P}_h^e(\mathbf{k}). \quad (26)$$

The quasiparticle propagator assumes the form [cf. Eq. (15) of [9]]

$$G^+(Q) = \sum_{h=r,\ell} \sum_{e=\pm} \frac{\mathcal{P}_h^e(\mathbf{q})}{q_0^2 - [\epsilon_q^e(\phi_h^e)]^2} [G_0^-(Q)]^{-1}, \quad (27)$$

where $\epsilon_q^e(\phi) \equiv \sqrt{(q-e\mu)^2 + |\phi|^2}$. From Eq. (26) of [9] we then infer that the gap equation (18) can be written in the form

$$\Phi^+(K) = \frac{2}{3} g^2 \frac{T}{V} \sum_Q \gamma^\mu \Delta_{\mu\nu}(K-Q) \times \sum_{h=r,\ell} \sum_{e=\pm} \frac{\phi_h^e(Q)}{q_0^2 - [\epsilon_q^e(\phi_h^e)]^2} \mathcal{P}_{-h}^{-e}(\mathbf{q}) \gamma^\nu, \quad (28)$$

where $-h=\ell$, if $h=r$, and $-h=r$, if $h=\ell$.

With the help of the projectors $\mathcal{P}_h^e(\mathbf{k})$ one can derive gap equations for the individual gap functions ϕ_h^e ,

$$\begin{aligned} \phi_h^e(K) = & \frac{2}{3} g^2 \frac{T}{V} \sum_Q \Delta_{\mu\nu}(K-Q) \\ & \times \left\{ \frac{\phi_h^e(Q)}{q_0^2 - [\epsilon_q^e(\phi_h^e)]^2} \text{Tr}[\mathcal{P}_h^e(\mathbf{k}) \gamma^\mu \mathcal{P}_{-h}^{-e}(\mathbf{q}) \gamma^\nu] \right. \\ & \left. + \frac{\phi_h^{-e}(Q)}{q_0^2 - [\epsilon_q^{-e}(\phi_h^{-e})]^2} \text{Tr}[\mathcal{P}_h^e(\mathbf{k}) \gamma^\mu \mathcal{P}_{-h}^{-e}(\mathbf{q}) \gamma^\nu] \right\}. \end{aligned} \quad (29)$$

To obtain this result we have used $\mathcal{P}_h \gamma^\mu = \gamma^\mu \mathcal{P}_{-h}$ and $\mathcal{P}_h \mathcal{P}_{-h} = 0$, so that the gap equations for right- and left-handed condensates decouple. This is a consequence of the

$U(1)_A$ symmetry of the QCD Lagrangian, which is expected to be effectively restored at asymptotically high densities [7,14].

In the Coulomb gauge, the HDL propagator is [23,24]

$$\Delta_{00}(P) = \Delta_l(P) + \xi_C \frac{P_0^2}{p^4}, \quad \Delta_{0i}(P) = \xi_C \frac{P_0 P_i}{p^4},$$

$$\Delta_{ij}(P) = (\delta_{ij} - \hat{p}_i \hat{p}_j) \Delta_l(P) + \xi_C \frac{\hat{p}_i \hat{p}_j}{p^2}. \quad (30)$$

We set the gauge parameter $\xi_C \equiv 0$. We shall show later that our results are manifestly gauge invariant to leading logarithmic accuracy. The longitudinal and transverse propagators $\Delta_{l,t}$ are defined in Eqs. (33) below.

The traces in Eq. (29) are readily evaluated. We need the terms

$$\text{Tr}[\mathcal{P}_h \Lambda^e(\mathbf{k}) \gamma_0 \Lambda^{\mp e}(\mathbf{q}) \gamma_0] = \frac{1 \pm \hat{\mathbf{k}} \cdot \hat{\mathbf{q}}}{2}, \quad (31a)$$

$$\sum_i \text{Tr}[\mathcal{P}_h \Lambda^e(\mathbf{k}) \gamma_i \Lambda^{\mp e}(\mathbf{q}) \gamma_i] = -\frac{3 \mp \hat{\mathbf{k}} \cdot \hat{\mathbf{q}}}{2}, \quad (31b)$$

$$\text{Tr}[\mathcal{P}_h \Lambda^e(\mathbf{k}) \boldsymbol{\gamma} \cdot \hat{\mathbf{p}} \Lambda^{\mp e}(\mathbf{q}) \boldsymbol{\gamma} \cdot \hat{\mathbf{p}}] = -\frac{1 \pm \hat{\mathbf{k}} \cdot \hat{\mathbf{q}}}{2} \frac{(k \mp q)^2}{p^2}, \quad (31c)$$

where $\mathbf{p} = \mathbf{k} - \mathbf{q}$. Obviously, the final result is independent of the chirality projector. We therefore conclude that the gap equations (29) for right- and left-handed gap functions are *identical*. This means that right- and left-handed gaps are equal up to a complex phase factor $\exp(i\theta)$. Condensation fixes the value of θ and breaks $U(1)_A$ spontaneously. As discussed in [7,14] this leads to spontaneous breaking of parity.

The gap equations for either right- or left-handed gap functions read

$$\phi_h^e(K) = \frac{2}{3} g^2 \frac{T}{V} \sum_Q \left\{ \frac{\phi_h^e(Q)}{q_0^2 - [\epsilon_q^e(\phi_h^e)]^2} \left[\Delta_l(K-Q) \frac{1 + \hat{\mathbf{k}} \cdot \hat{\mathbf{q}}}{2} + \Delta_l(K-Q) \left(-\frac{3 - \hat{\mathbf{k}} \cdot \hat{\mathbf{q}}}{2} + \frac{1 + \hat{\mathbf{k}} \cdot \hat{\mathbf{q}}}{2} \frac{(k-q)^2}{(\mathbf{k}-\mathbf{q})^2} \right) \right] \right. \\ \left. + \frac{\phi_h^{-e}(Q)}{q_0^2 - [\epsilon_q^{-e}(\phi_h^{-e})]^2} \left[\Delta_l(K-Q) \frac{1 - \hat{\mathbf{k}} \cdot \hat{\mathbf{q}}}{2} + \Delta_l(K-Q) \left(-\frac{3 + \hat{\mathbf{k}} \cdot \hat{\mathbf{q}}}{2} + \frac{1 - \hat{\mathbf{k}} \cdot \hat{\mathbf{q}}}{2} \frac{(k+q)^2}{(\mathbf{k}-\mathbf{q})^2} \right) \right] \right\}. \quad (32)$$

The gap equations involve singularities from both the quark and gluon propagators. The poles of $1/\{q_0^2 - [\epsilon_q^e(\phi_h^e)]^2\}$ give a residue $\sim 1/\epsilon_q^e(\phi_h^e)$. Remember, though, that the quasipar-

ticle energy ϵ_q^+ is very small near the Fermi surface, $\epsilon_\mu^+ = |\phi_h^+|$. The quasi-antiparticle energy ϵ_q^- , however, is always larger than μ . Therefore, in weak coupling, the dominant terms arise from the quasiparticle poles $q_0 = \pm \epsilon_q^+(\phi_h^+)$ [9], and the contribution from quasi-antiparticle poles can be neglected. Consequently, we do not need to solve Eq. (32) for the quasi-antiparticle gaps, ϕ_h^- , in order to determine the solution for the quasiparticle gaps, ϕ_h^+ . In the following, we drop the subscript h and superscript $+$ to simplify the notation, and denote $\phi_h^+(K) \equiv \phi(K)$.

D. Spectral representations

To perform the Matsubara sum over quark energies $q_0 = -i(2n+1)\pi T$, we introduce spectral representations. For the gluon propagators [23,24],

$$\Delta_l(P) \equiv -\frac{1}{p^2} + \int_0^{1/T} d\tau e^{p_0 \tau} \Delta_l(\tau, \mathbf{p}),$$

$$\Delta_t(P) \equiv \int_0^{1/T} d\tau e^{p_0 \tau} \Delta_t(\tau, \mathbf{p}), \quad (33a)$$

$$\Delta_{l,t}(\tau, \mathbf{p}) \equiv \int_0^\infty d\omega \rho_{l,t}(\omega, \mathbf{p}) \{ [1 + n_B(\omega/T)] e^{-\omega \tau} + n_B(\omega/T) e^{\omega \tau} \}, \quad (33b)$$

where $n_B(x) \equiv 1/(e^x - 1)$ is the Bose-Einstein distribution function. The term $-1/p^2$ in the longitudinal propagator cancels the contribution of $\Delta_l(P)$ at $p_0 \rightarrow \infty$ [24]. The spectral densities are given by [23,24]

$$\rho_{l,t}(\omega, \mathbf{p}) = \rho_{l,t}^{\text{pole}}(\omega, \mathbf{p}) \delta[\omega - \omega_{l,t}(\mathbf{p})] + \rho_{l,t}^{\text{cut}}(\omega, \mathbf{p}) \theta(p - \omega), \quad (34a)$$

$$\rho_l^{\text{pole}}(\omega, \mathbf{p}) = \frac{\omega(\omega^2 - p^2)}{p^2(p^2 + 3m_g^2 - \omega^2)}, \quad (34b)$$

$$\rho_l^{\text{cut}}(\omega, \mathbf{p}) = \frac{2M^2}{\pi} \frac{\omega}{p} \left\{ \left[p^2 + 3m_g^2 \left(1 - \frac{\omega}{2p} \ln \left| \frac{p+\omega}{p-\omega} \right| \right) \right]^2 + \left(2M^2 \frac{\omega}{p} \right)^2 \right\}^{-1}, \quad (34c)$$

$$\rho_t^{\text{pole}}(\omega, \mathbf{p}) = \frac{\omega(\omega^2 - p^2)}{3m_g^2 \omega^2 - (\omega^2 - p^2)^2}, \quad (34d)$$

$$\rho_t^{\text{cut}}(\omega, \mathbf{p}) = \frac{M^2}{\pi} \frac{\omega}{p} \frac{p^2}{p^2 - \omega^2} \left\{ \left[p^2 + \frac{3}{2} m_g^2 \left(\frac{\omega^2}{p^2 - \omega^2} + \frac{\omega}{2p} \ln \left| \frac{p+\omega}{p-\omega} \right| \right) \right]^2 + \left(M^2 \frac{\omega}{p} \right)^2 \right\}^{-1}. \quad (34e)$$

The basic parameter of the HDL propagators is the gluon mass

$$m_g^2 \equiv N_f \frac{g^2 \mu^2}{6\pi^2} + \left(N_c + \frac{N_f}{2} \right) \frac{g^2 T^2}{9}. \quad (35)$$

We also found it convenient to introduce

$$M^2 \equiv \frac{3\pi}{4} m_g^2 \simeq 2.36 m_g^2. \quad (36)$$

The functions $\omega_{l,t}(\mathbf{p})$ are the solutions of the equations

$$p^2 + 3m_g^2 \left[1 - \frac{\omega_l}{2p} \ln \left(\frac{\omega_l + p}{\omega_l - p} \right) \right] = 0, \quad (37a)$$

$$p^2(\omega_t^2 - p^2) - \frac{3}{2} m_g^2 \left[\omega_t + \frac{\omega_t}{2p} (p^2 - \omega_t^2) \ln \left(\frac{\omega_t + p}{\omega_t - p} \right) \right] = 0, \quad (37b)$$

and define the dispersion relations for longitudinal and transverse gluons, respectively. They satisfy $\omega_{l,t}(\mathbf{p}) \geq m_g$.

We argue later that the phase-space region which dominates the gap integrals is the nearly static, small-momentum limit. The gluon energies are on the order of the gap, $\omega \sim \phi$, while the gluon momenta p are much larger than ω , but much smaller than m_g . In this limit, $\omega \ll p \ll m_g$,

$$\begin{aligned} \rho_l^{\text{cut}}(\omega, \mathbf{p}) &\simeq \frac{2M^2}{\pi} \frac{\omega}{p} \frac{1}{(p^2 + 3m_g^2)^2} \\ \rho_t^{\text{cut}}(\omega, \mathbf{p}) &\simeq \frac{M^2}{\pi} \frac{\omega p}{p^6 + (M^2 \omega)^2}. \end{aligned} \quad (38)$$

We also introduce a spectral representation for the quantity

$$\Xi(Q) \equiv \frac{\phi(Q)}{q_0^2 - [\epsilon_q(\phi)]^2} \equiv \int_0^{1/T} d\tau e^{q_0 \tau} \Xi(\tau, \mathbf{q}). \quad (39)$$

Neglecting the singularities of $\phi(Q)$ in the complex q_0 plane, and assuming $\phi(q_0, \mathbf{q})$ to be an even function of q_0 , we find

$$\begin{aligned} \Xi(\tau, \mathbf{q}) &\equiv \int_0^\infty d\omega \tilde{\rho}(\omega, \mathbf{q}) \{ [1 - n_F(\omega/T)] e^{-\omega\tau} \\ &\quad - n_F(\omega/T) e^{\omega\tau} \}, \end{aligned} \quad (40)$$

where

$$\tilde{\rho}(\omega, \mathbf{q}) \equiv - \frac{\phi(\omega, \mathbf{q})}{2\omega} \delta(\omega - \epsilon_q), \quad \epsilon_q \equiv \epsilon_q(\phi), \quad (41)$$

and $n_F(x) = 1/(e^x + 1)$ is the Fermi-Dirac distribution function.

By neglecting the singularities of $\phi(Q)$, the only contribution to the spectral representation of $\Xi(Q)$ is from the poles of $1/\{q_0^2 - [\epsilon_q(\phi)]^2\}$, which generates the delta function in the spectral density (41). This forces the energy in the gap function $\phi(q_0, \mathbf{q})$ to lie on the quasiparticle mass shell, $q_0 = \epsilon_q(\phi)$.

The Matsubara sums over q_0 can now be computed as ($\mathbf{p} \equiv \mathbf{k} - \mathbf{q}$)

$$\begin{aligned} T \sum_{q_0} \Delta_l(K-Q) \Xi(Q) &= - \frac{\phi(\epsilon_q, \mathbf{q})}{2\epsilon_q} \left\{ - \frac{1}{2} \tanh \left(\frac{\epsilon_q}{2T} \right) \frac{2}{p^2} + \int_0^\infty d\omega \rho_l(\omega, \mathbf{p}) \left[\frac{1}{2} \tanh \left(\frac{\epsilon_q}{2T} \right) \left(\frac{1}{k_0 + \omega + \epsilon_q} - \frac{1}{k_0 - \omega - \epsilon_q} \right. \right. \right. \\ &\quad \left. \left. - \frac{1}{k_0 - \omega + \epsilon_q} + \frac{1}{k_0 + \omega - \epsilon_q} \right) + \frac{1}{2} \coth \left(\frac{\omega}{2T} \right) \left(\frac{1}{k_0 + \omega + \epsilon_q} - \frac{1}{k_0 - \omega - \epsilon_q} + \frac{1}{k_0 - \omega + \epsilon_q} \right. \right. \\ &\quad \left. \left. - \frac{1}{k_0 + \omega - \epsilon_q} \right) \right] \right\}, \end{aligned} \quad (42a)$$

$$\begin{aligned} T \sum_{q_0} \Delta_t(K-Q) \Xi(Q) &= - \frac{\phi(\epsilon_q, \mathbf{q})}{2\epsilon_q} \int_0^\infty d\omega \rho_t(\omega, \mathbf{p}) \left[\frac{1}{2} \tanh \left(\frac{\epsilon_q}{2T} \right) \left(\frac{1}{k_0 + \omega + \epsilon_q} - \frac{1}{k_0 - \omega - \epsilon_q} - \frac{1}{k_0 - \omega + \epsilon_q} + \frac{1}{k_0 + \omega - \epsilon_q} \right) \right. \\ &\quad \left. + \frac{1}{2} \coth \left(\frac{\omega}{2T} \right) \left(\frac{1}{k_0 + \omega + \epsilon_q} - \frac{1}{k_0 - \omega - \epsilon_q} + \frac{1}{k_0 - \omega + \epsilon_q} - \frac{1}{k_0 + \omega - \epsilon_q} \right) \right], \end{aligned} \quad (42b)$$

where we have made use of Eq. (41) and $e^{k_0/T} \equiv -1$, since $k_0 = -i(2n+1)\pi T$.

E. Analytic continuation

In field theories, the only physical quantities are those on the mass shell, such as S -matrix elements. In our case, this implies that we need the gap function not for Euclidean val-

ues of the energy, $k_0 = -i(2n+1)\pi T$, but on the quasiparticle mass shell, for real values of $k_0 = \epsilon_k$. This is achieved by analytically continuing $k_0 \rightarrow \epsilon_k + i\eta$ [2]. The analytic continuation of the gap equation (32) introduces a term $i\eta$ in the energy denominators in Eq. (42). As $1/(x+i\eta) \equiv \text{P}(1/x) - i\pi\delta(x)$ (where P stands for the principal value), this generates an imaginary part for the function $\phi(\epsilon_k, \mathbf{k})$. As shown below, this imaginary part is down by g relative to the real

part. This justifies neglecting the singularities of $\phi(Q)$ in deriving Eq. (42). In the following, implicitly we take the principal value of all energy denominators. Finally, since the gap function $\phi(k_0, \mathbf{k})$ does not depend on the orientation of the 3-vector \mathbf{k} , but only on its magnitude, k [cf. Eq. (32)], the on-shell gap function is a function of k only, $\phi(\epsilon_k, \mathbf{k}) \equiv \phi(\epsilon_k, k) \equiv \phi_k$.

F. Contribution from longitudinal gluons

The contribution from longitudinal gluons is given by Eq. (42a). In general, this equation can only be evaluated numerically, using the full expressions (34) for the spectral densities. We can proceed analytically by noting that, due to the factor $1/\epsilon_q$, the integral over momenta \mathbf{q} is dominated by the region close to the Fermi surface. In the following, we shall therefore assume that the momenta \mathbf{k} and \mathbf{q} are close to the Fermi surface, such that $\epsilon_k \sim \epsilon_q \ll m_g$. Now rewrite

$$\begin{aligned} & \frac{1}{\omega + \epsilon_q + \epsilon_k} + \frac{1}{\omega + \epsilon_q - \epsilon_k} + \frac{1}{\omega - (\epsilon_q + \epsilon_k)} + \frac{1}{\omega - (\epsilon_q - \epsilon_k)} \\ &= \frac{1}{\omega} \left[4 - \frac{\epsilon_q + \epsilon_k}{\omega + \epsilon_q + \epsilon_k} - \frac{\epsilon_q - \epsilon_k}{\omega + \epsilon_q - \epsilon_k} + \frac{\epsilon_q + \epsilon_k}{\omega - (\epsilon_q + \epsilon_k)} \right. \\ & \quad \left. + \frac{\epsilon_q - \epsilon_k}{\omega - (\epsilon_q - \epsilon_k)} \right], \end{aligned} \quad (43)$$

and make use of the sum rule [23,24]

$$2 \int_0^\infty d\omega \frac{\rho_l(\omega, \mathbf{p})}{\omega} = \frac{1}{p^2} + \Delta_l(0, \mathbf{p}), \quad \Delta_l(0, \mathbf{p}) \equiv -\frac{1}{p^2 + 3m_g^2}, \quad (44)$$

to obtain

$$\begin{aligned} & T \sum_{q_0} \Delta_l(K-Q) \Xi(Q) \\ &= -\frac{\phi(\epsilon_q, \mathbf{q})}{2\epsilon_q} \left\{ \frac{1}{2} \tanh\left(\frac{\epsilon_q}{2T}\right) \left[-\frac{2}{p^2 + 3m_g^2} + \mathcal{J}_l(\mathbf{k}, \mathbf{q}) \right] \right. \\ & \quad \left. + \mathcal{K}_l(\mathbf{k}, \mathbf{q}) \right\}, \end{aligned} \quad (45)$$

where

$$\begin{aligned} \mathcal{J}_l(\mathbf{k}, \mathbf{q}) &\equiv \int_0^\infty d\omega \frac{\rho_l(\omega, \mathbf{p})}{\omega} \left[\frac{\epsilon_q + \epsilon_k}{\omega - (\epsilon_q + \epsilon_k)} - \frac{\epsilon_q + \epsilon_k}{\omega + \epsilon_q + \epsilon_k} \right. \\ & \quad \left. + \frac{\epsilon_q - \epsilon_k}{\omega - (\epsilon_q - \epsilon_k)} - \frac{\epsilon_q - \epsilon_k}{\omega + \epsilon_q - \epsilon_k} \right] \end{aligned} \quad (46)$$

and

$$\begin{aligned} \mathcal{K}_l(\mathbf{k}, \mathbf{q}) &\equiv \int_0^\infty d\omega \rho_l(\omega, \mathbf{p}) \frac{1}{2} \coth\left(\frac{\omega}{2T}\right) \left[\frac{1}{\omega + \epsilon_q + \epsilon_k} \right. \\ & \quad \left. + \frac{1}{\omega + \epsilon_q - \epsilon_k} - \frac{1}{\omega - (\epsilon_q + \epsilon_k)} - \frac{1}{\omega - (\epsilon_q - \epsilon_k)} \right]. \end{aligned} \quad (47)$$

The integral \mathcal{J}_l consists of two parts, one from the pole term in the spectral density, and one from the cut term. The pole term is

$$\begin{aligned} \mathcal{J}_l^{\text{pole}}(\mathbf{k}, \mathbf{q}) &= \frac{1}{p^2} \frac{\omega_l^2 - p^2}{p^2 + 3m_g^2 - \omega_l^2} \left[\frac{\epsilon_q + \epsilon_k}{\omega_l - (\epsilon_q + \epsilon_k)} - \frac{\epsilon_q + \epsilon_k}{\omega_l + \epsilon_q + \epsilon_k} \right. \\ & \quad \left. + \frac{\epsilon_q - \epsilon_k}{\omega_l - (\epsilon_q - \epsilon_k)} - \frac{\epsilon_q - \epsilon_k}{\omega_l + \epsilon_q - \epsilon_k} \right]. \end{aligned} \quad (48)$$

As $\omega_l \geq m_g \gg \epsilon_k \sim \epsilon_q$, we may expand the energy denominators around ω_l ,

$$\mathcal{J}_l^{\text{pole}}(\mathbf{k}, \mathbf{q}) \simeq \frac{1}{p^2} \frac{\omega_l^2 - p^2}{p^2 + 3m_g^2 - \omega_l^2} 4 \frac{\epsilon_q^2 + \epsilon_k^2}{\omega_l^2}. \quad (49)$$

This contribution is quadratic in $\epsilon_q/\omega_l \sim \epsilon_k/\omega_l \ll 1$ and thus negligible.

The cut term is estimated using the approximate form of the spectral density (38),

$$\begin{aligned} \mathcal{J}_l^{\text{cut}}(\mathbf{k}, \mathbf{q}) &\simeq \frac{2M^2}{\pi p} \frac{1}{(p^2 + 3m_g^2)^2} \int_0^p d\omega \left[\frac{\epsilon_q + \epsilon_k}{\omega - (\epsilon_q + \epsilon_k)} \right. \\ & \quad \left. - \frac{\epsilon_q + \epsilon_k}{\omega + \epsilon_q + \epsilon_k} + \frac{\epsilon_q - \epsilon_k}{\omega - (\epsilon_q - \epsilon_k)} - \frac{\epsilon_q - \epsilon_k}{\omega + \epsilon_q - \epsilon_k} \right] \\ &= \frac{2M^2}{\pi p} \frac{1}{(p^2 + 3m_g^2)^2} \left[(\epsilon_q + \epsilon_k) \ln \left| \frac{\epsilon_q + \epsilon_k - p}{\epsilon_q + \epsilon_k + p} \right| \right. \\ & \quad \left. + (\epsilon_q - \epsilon_k) \ln \left| \frac{\epsilon_q - \epsilon_k - p}{\epsilon_q - \epsilon_k + p} \right| \right]. \end{aligned} \quad (50)$$

This integral is proportional to factors $\epsilon_q \pm \epsilon_k$, which parametrically cancel the prefactor $1/\epsilon_q$ in Eq. (45). (This is true except for $p \rightarrow 0$, where these factors cancel when expanding the logarithms. However, the Jacobian of the angular integration in the gap equation, $\int d\cos\theta \sim \int dp$, suppresses this contribution.) It is thus negligible compared to the term $\sim 2/(p^2 + 3m_g^2)$ in Eq. (45).

We now turn to evaluate $\mathcal{K}_l(\mathbf{k}, \mathbf{q})$. After expanding the energy denominators in Eq. (47) around $\omega_l \geq m_g \gg \epsilon_k \sim \epsilon_q$, the pole part reads

$$\mathcal{K}_l^{\text{pole}}(\mathbf{k}, \mathbf{q}) \simeq -\frac{1}{p^2} \frac{\omega_l^2 - p^2}{p^2 + 3m_g^2 - \omega_l^2} \frac{1}{2} \coth\left(\frac{\omega_l}{2T}\right) 4 \frac{\epsilon_q}{\omega_l}. \quad (51)$$

The range of temperatures of interest is limited by T_c , the critical temperature for the onset of color superconductivity.

As $T_c \sim \phi_0 \ll m_g \ll \omega_l$, $\coth(\omega/2T) \sim 1$. The factor ϵ_q cancels the prefactor in Eq. (45), such that $\mathcal{K}_l^{\text{pole}}$ is negligible compared to the term $\sim 2/(p^2 + 3m_g^2)$ in Eq. (45).

To estimate the cut term, we use the approximate expression (38), and employ a relation similar to Eq. (43),

$$\begin{aligned} & \frac{1}{\omega + \epsilon_q + \epsilon_k} + \frac{1}{\omega + \epsilon_q - \epsilon_k} - \frac{1}{\omega - (\epsilon_q + \epsilon_k)} - \frac{1}{\omega - (\epsilon_q - \epsilon_k)} \\ &= -\frac{1}{\omega} \left[\frac{\epsilon_q + \epsilon_k}{\omega + \epsilon_q + \epsilon_k} + \frac{\epsilon_q - \epsilon_k}{\omega + \epsilon_q - \epsilon_k} \right. \\ & \quad \left. + \frac{\epsilon_q + \epsilon_k}{\omega - (\epsilon_q + \epsilon_k)} + \frac{\epsilon_q - \epsilon_k}{\omega - (\epsilon_q - \epsilon_k)} \right], \end{aligned} \quad (52)$$

to obtain

$$\begin{aligned} \mathcal{K}_l^{\text{cut}}(\mathbf{k}, \mathbf{q}) &\simeq -\frac{2M^2}{\pi p} \frac{1}{(p^2 + 3m_g^2)^2} \int_0^p d\omega \frac{1}{2} \coth\left(\frac{\omega}{2T}\right) \\ & \quad \times \left[\frac{\epsilon_q + \epsilon_k}{\omega + \epsilon_q + \epsilon_k} + \frac{\epsilon_q - \epsilon_k}{\omega + \epsilon_q - \epsilon_k} + \frac{\epsilon_q + \epsilon_k}{\omega - (\epsilon_q + \epsilon_k)} \right. \\ & \quad \left. + \frac{\epsilon_q - \epsilon_k}{\omega - (\epsilon_q - \epsilon_k)} \right]. \end{aligned} \quad (53)$$

For ω of order T or larger, this contribution is small, since then $\coth(\omega/2T) \sim 1$, and thus all terms are proportional to $\epsilon_q \pm \epsilon_k$. For $\omega \ll T$, however, the large (classical) occupation number density of gluons can enhance this contribution. In the classical limit, one approximates $\coth(\omega/2T) \simeq 2T/\omega$. Simultaneously, as the range of validity of this approximation is $\omega \ll T$, the upper limit of the integral should now be replaced by $p^* \equiv \min(T, p)$. Reverting the step (52), we obtain

$$\begin{aligned} \mathcal{K}_l^{\text{cut}}(\mathbf{k}, \mathbf{q}) &\simeq \frac{2M^2 T}{\pi p} \frac{1}{(p^2 + 3m_g^2)^2} \\ & \quad \times \ln \left| \frac{p^* + \epsilon_q + \epsilon_k}{p^* - (\epsilon_q + \epsilon_k)} \frac{p^* + \epsilon_q - \epsilon_k}{p^* - (\epsilon_q - \epsilon_k)} \right|. \end{aligned} \quad (54)$$

For $T \rightarrow 0$, we may expand the logarithm to show that this contribution is quadratically small in T . On the other hand, for $T \rightarrow T_c$, close to the Fermi surface $\epsilon_q \sim \epsilon_k \sim \phi \rightarrow 0$, and the logarithm can be expanded for $p^* \gg \epsilon_q \pm \epsilon_k$. The result is proportional to $\epsilon_q \pm \epsilon_k$, which cancels the prefactor $1/\epsilon_q$, and thus suppresses this contribution. We shall therefore neglect it in the following.

The final result for the longitudinal contribution is thus

$$T \sum_{q_0} \Delta_l(K-Q) \Xi(Q) \simeq \frac{\phi(\epsilon_q, \mathbf{q})}{2\epsilon_q} \frac{1}{2} \tanh\left(\frac{\epsilon_q}{2T}\right) \frac{2}{p^2 + 3m_g^2}. \quad (55)$$

This result could also have been obtained by simply taking the static limit of the longitudinal gluon propagator, $\Delta_l(0, \mathbf{p})$, on the left-hand side in Eq. (55), and performing the Matsubara sum directly. We conclude that the contribution of

static electric gluons dominates over that of nonstatic electric gluons. We note that, while the individual terms (49) and (51) exhibit an apparent infrared divergent prefactor $1/p^2$, the sum of all terms is infrared finite, as can be shown by computing the contribution of electric gluons without using Eq. (43).

G. Contribution from transverse gluons

The contribution from transverse gluons is written in a form similar to Eq. (45):

$$\begin{aligned} T \sum_{q_0} \Delta_t(K-Q) \Xi(Q) &= -\frac{\phi(\epsilon_q, \mathbf{q})}{2\epsilon_q} \left[\frac{1}{2} \tanh\left(\frac{\epsilon_q}{2T}\right) \mathcal{J}_t(\mathbf{k}, \mathbf{q}) \right. \\ & \quad \left. + \mathcal{K}_t(\mathbf{k}, \mathbf{q}) \right], \end{aligned} \quad (56)$$

where

$$\begin{aligned} \mathcal{J}_t(\mathbf{k}, \mathbf{q}) &\equiv \int_0^\infty d\omega \rho_t(\omega, \mathbf{p}) \left[\frac{1}{\omega + \epsilon_q + \epsilon_k} + \frac{1}{\omega + \epsilon_q - \epsilon_k} \right. \\ & \quad \left. + \frac{1}{\omega - (\epsilon_q + \epsilon_k)} + \frac{1}{\omega - (\epsilon_q - \epsilon_k)} \right] \end{aligned} \quad (57)$$

and

$$\begin{aligned} \mathcal{K}_t(\mathbf{k}, \mathbf{q}) &\equiv \int_0^\infty d\omega \rho_t(\omega, \mathbf{p}) \frac{1}{2} \coth\left(\frac{\omega}{2T}\right) \left[\frac{1}{\omega + \epsilon_q + \epsilon_k} \right. \\ & \quad \left. + \frac{1}{\omega + \epsilon_q - \epsilon_k} - \frac{1}{\omega - (\epsilon_q + \epsilon_k)} - \frac{1}{\omega - (\epsilon_q - \epsilon_k)} \right]. \end{aligned} \quad (58)$$

The function \mathcal{J}_t consists of a pole and a cut term. In the first, we expand the energy denominators around $\omega_t \geq m_g \gg \epsilon_q \sim \epsilon_k$, to obtain, to leading order in $\epsilon_q \pm \epsilon_k$,

$$\mathcal{J}_t^{\text{pole}}(\mathbf{k}, \mathbf{q}) \simeq 4 \frac{\omega_t^2 - p^2}{3m_g^2 \omega_t^2 - (\omega_t^2 - p^2)^2}. \quad (59)$$

For the cut term, we again employ Eq. (38) to obtain

$$\begin{aligned} \mathcal{J}_t^{\text{cut}}(\mathbf{k}, \mathbf{q}) &\simeq \frac{M^2 p}{\pi} \int_0^p d\omega \frac{\omega}{p^6 + (M^2 \omega)^2} \left[\frac{1}{\omega + \epsilon_q + \epsilon_k} \right. \\ & \quad \left. + \frac{1}{\omega + \epsilon_q - \epsilon_k} + \frac{1}{\omega - (\epsilon_q + \epsilon_k)} + \frac{1}{\omega - (\epsilon_q - \epsilon_k)} \right]. \end{aligned} \quad (60)$$

The ω integral can be performed analytically. Denote $a \equiv p^3/M^2$. Then

$$\begin{aligned}
 \mathcal{J}_t^{\text{cut}}(\mathbf{k}, \mathbf{q}) &\simeq \frac{p}{\pi M^2} \int_0^p d\omega \frac{\omega}{\omega^2 + a^2} \left[\frac{1}{\omega + \epsilon_q + \epsilon_k} + \frac{1}{\omega + \epsilon_q - \epsilon_k} \right. \\
 &\quad \left. + \frac{1}{\omega - (\epsilon_q + \epsilon_k)} + \frac{1}{\omega - (\epsilon_q - \epsilon_k)} \right] \\
 &= \frac{p}{\pi M^2} \left\{ 2 \left[\frac{a}{a^2 + (\epsilon_q + \epsilon_k)^2} \right. \right. \\
 &\quad \left. \left. + \frac{a}{a^2 + (\epsilon_q - \epsilon_k)^2} \right] \arctan\left(\frac{p}{a}\right) \right. \\
 &\quad \left. - \frac{\epsilon_q + \epsilon_k}{a^2 + (\epsilon_q + \epsilon_k)^2} \ln \left| \frac{p + \epsilon_q + \epsilon_k}{p - (\epsilon_q + \epsilon_k)} \right| \right. \\
 &\quad \left. - \frac{\epsilon_q - \epsilon_k}{a^2 + (\epsilon_q - \epsilon_k)^2} \ln \left| \frac{p + \epsilon_q - \epsilon_k}{p - (\epsilon_q - \epsilon_k)} \right| \right\}. \quad (61)
 \end{aligned}$$

The terms proportional to $\epsilon_q \pm \epsilon_k$ are of higher order and can be neglected, such that

$$\begin{aligned}
 \mathcal{J}_t^{\text{cut}}(\mathbf{k}, \mathbf{q}) &\simeq \left[\frac{p^4}{p^6 + M^4(\epsilon_q + \epsilon_k)^2} \right. \\
 &\quad \left. + \frac{p^4}{p^6 + M^4(\epsilon_q - \epsilon_k)^2} \right] \frac{2}{\pi} \arctan\left(\frac{M^2}{p^2}\right). \quad (62)
 \end{aligned}$$

The arctan cuts \mathcal{J}_t off for momenta p larger than $\sim M$. To make further progress, in the following we replace the more complicated arctan with a simple θ function cutoff, $2 \arctan(M^2/p^2)/\pi \rightarrow \theta(M-p)$. However, to retain consistency with the sum rule [23,24]

$$2 \int_0^\infty d\omega \frac{\rho_t(\omega, \mathbf{p})}{\omega} = \frac{1}{p^2}, \quad (63)$$

we also have to modify the result for the pole term (59). To enact the modification, note that $\mathcal{J}_t/2$ is identical to the left-hand side of the sum rule (63), when we set $\epsilon_q = \epsilon_k = 0$ in Eq. (57). Thus, the most simple choice is

$$\mathcal{J}_t^{\text{pole}}(\mathbf{k}, \mathbf{q}) \simeq \frac{2}{p^2} \theta(p-M), \quad (64)$$

since then, for $\epsilon_q = \epsilon_k = 0$,

$$\mathcal{J}_t(\mathbf{k}, \mathbf{q}) = \mathcal{J}_t^{\text{pole}}(\mathbf{k}, \mathbf{q}) + \mathcal{J}_t^{\text{cut}}(\mathbf{k}, \mathbf{q}) \equiv \frac{2}{p^2}. \quad (65)$$

The function \mathcal{K}_t also consists of a pole and a cut term. In the first, we expand the energy denominators around $\omega_t \gg m_g \gg \epsilon_q \sim \epsilon_k$,

$$\mathcal{K}_t^{\text{pole}}(\mathbf{k}, \mathbf{q}) \simeq - \frac{\omega_t^2 - p^2}{3m_g^2 \omega_t^2 - (\omega_t^2 - p^2)^2} \frac{1}{2} \coth\left(\frac{\omega_t}{2T}\right) \frac{4\epsilon_q}{\omega_t}. \quad (66)$$

As the factor ϵ_q cancels the prefactor $1/\epsilon_q$ in Eq. (56), this contribution is of higher order and thus negligible.

The cut term is estimated with Eq. (38) to be (as before, $a = p^3/M^2$)

$$\begin{aligned}
 \mathcal{K}_t^{\text{cut}}(\mathbf{k}, \mathbf{q}) &\simeq \frac{p}{\pi M^2} \int_0^p d\omega \frac{\omega}{\omega^2 + a^2} \frac{1}{2} \coth\left(\frac{\omega}{2T}\right) \left[\frac{1}{\omega + \epsilon_q + \epsilon_k} \right. \\
 &\quad \left. + \frac{1}{\omega + \epsilon_q - \epsilon_k} - \frac{1}{\omega - (\epsilon_q + \epsilon_k)} - \frac{1}{\omega - (\epsilon_q - \epsilon_k)} \right]. \quad (67)
 \end{aligned}$$

For ω of order T or larger, $\coth(\omega/2T) \simeq 1$, similar steps that led to Eq. (61) now show that the final result is proportional to $\epsilon_q \pm \epsilon_k$, and thus of higher order. For $\omega \ll T$, however,

$$\begin{aligned}
 \mathcal{K}_t^{\text{cut}}(\mathbf{k}, \mathbf{q}) &\simeq \frac{pT}{\pi M^2} \int_0^{p^*} d\omega \frac{1}{\omega^2 + a^2} \left[\frac{1}{\omega + \epsilon_q + \epsilon_k} + \frac{1}{\omega + \epsilon_q - \epsilon_k} \right. \\
 &\quad \left. - \frac{1}{\omega - (\epsilon_q + \epsilon_k)} - \frac{1}{\omega - (\epsilon_q - \epsilon_k)} \right] \\
 &\simeq \frac{M^2}{\pi} \left[\frac{pT}{p^6 + M^4(\epsilon_q + \epsilon_k)^2} \ln \left| \frac{p^* + \epsilon_q + \epsilon_k}{p^* - (\epsilon_q + \epsilon_k)} \right| \right. \\
 &\quad \left. + \frac{pT}{p^6 + M^4(\epsilon_q - \epsilon_k)^2} \ln \left| \frac{p^* + \epsilon_q - \epsilon_k}{p^* - (\epsilon_q - \epsilon_k)} \right| \right], \quad (68)
 \end{aligned}$$

where as before $p^* = \min(T, p)$, and terms proportional to $\epsilon_q \pm \epsilon_k$ have been neglected in the last line. For small T , an expansion of the logarithms shows that this contribution is quadratic in T . On the other hand, for $T \rightarrow T_c$, an expansion of the logarithms for $p^* \gg \epsilon_q \pm \epsilon_k$ shows that it is proportional to $\epsilon_q \pm \epsilon_k$; it thus parametrically cancels the prefactor $1/\epsilon_q$. We shall thus neglect this contribution in the following.

Our final result for the transverse contribution is therefore

$$\begin{aligned}
 T \sum_{q_0} \Delta_t(K-Q) \Xi(Q) &\simeq - \frac{\phi(\epsilon_q, \mathbf{q})}{2\epsilon_q} \frac{1}{2} \tanh\left(\frac{\epsilon_q}{2T}\right) \left\{ \frac{2}{p^2} \theta(p-M) + \theta(M-p) \right. \\
 &\quad \left. \times \left[\frac{p^4}{p^6 + M^4(\epsilon_q + \epsilon_k)^2} + \frac{p^4}{p^6 + M^4(\epsilon_q - \epsilon_k)^2} \right] \right\}. \quad (69)
 \end{aligned}$$

H. Gap equation

Collecting the results from the previous subsections, and replacing the angular integration $\int d \cos \theta$ by an integral over $p = |\mathbf{k} - \mathbf{q}|$, the gap equation (32) reads

$$\begin{aligned}
\phi_k &= \frac{g^2}{24\pi^2 k} \int_{\mu-\delta}^{\mu+\delta} dq \frac{q}{\epsilon_q} \tanh\left(\frac{\epsilon_q}{2T}\right) \phi_q \\
&\times \int_{|k-q|}^{k+q} dp p \left\{ \frac{2}{p^2 + 3m_g^2} \frac{(k+q)^2 - p^2}{4kq} + \left[\frac{2}{p^2} \theta(p-M) \right. \right. \\
&+ \left. \left. \theta(M-p) \left(\frac{p^4}{p^6 + M^4(\epsilon_q + \epsilon_k)^2} + \frac{p^4}{p^6 + M^4(\epsilon_q - \epsilon_k)^2} \right) \right] \right\} \\
&\times \left(1 + \frac{p^2}{4kq} - \frac{(k^2 - q^2)^2}{4kqp^2} \right). \quad (70)
\end{aligned}$$

Here, we restricted the q integration to a region $\mu - \delta \leq q \leq \mu + \delta$, $\delta \ll \mu$ around the Fermi surface, since we assumed that $\epsilon_q \sim \epsilon_k \leq m_g \sim g\mu \ll \mu$. Therefore, we may set $k \approx q \sim \mu$. Also, to leading order we may neglect p^2 terms with respect to $(k+q)^2$ terms. Then, the gap equation (70) simplifies to

$$\begin{aligned}
\phi_k &\approx \frac{g^2}{24\pi^2} \int_{\mu-\delta}^{\mu+\delta} dq \frac{q}{\epsilon_q} \tanh\left(\frac{\epsilon_q}{2T}\right) \phi_q \left[\ln\left(\frac{4\mu^2}{3m_g^2}\right) + \ln\left(\frac{4\mu^2}{M^2}\right) \right. \\
&+ \left. \frac{1}{3} \ln\left(\frac{M^2}{|\epsilon_q^2 - \epsilon_k^2|}\right) \right]. \quad (71)
\end{aligned}$$

The first term in brackets, $\sim \ln(4\mu^2/3m_g^2)$, arises from static electric gluons [proportional to $2/(p^2 + 3m_g^2)$ in Eq. (70)], the second, $\sim \ln(4\mu^2/M^2)$, from nonstatic magnetic gluons [proportional to $\theta(p-M)$ in Eq. (70)], and the last term, $\sim \ln(M^2/|\epsilon_q^2 - \epsilon_k^2|)$, from soft, Landau-damped magnetic gluons [proportional to $\theta(M-p)$ in Eq. (70)]. These terms can be combined to give

$$\phi_k \approx \frac{g^2}{18\pi^2} \int_0^{\delta} d(q-\mu) \frac{1}{\epsilon_q} \tanh\left(\frac{\epsilon_q}{2T}\right) \frac{1}{2} \ln\left(\frac{b^2 \mu^2}{|\epsilon_q^2 - \epsilon_k^2|}\right) \phi_q, \quad (72)$$

where we exploited the symmetry of the integrand in Eq. (71) around the Fermi surface to restrict the $q - \mu$ integration to the interval $\mu \leq q \leq \mu + \delta$; i.e., we only integrate over momenta q from the Fermi surface up to $\mu + \delta$. Moreover, we have defined

$$b \equiv 256\pi^4 \left(\frac{2}{N_f g^2} \right)^{5/2}. \quad (73)$$

The temperature dependence of m_g [cf. Eq. (35)], has been neglected, as $T \sim \phi_0 \ll m_g \sim g\mu$.

The result (73) for b agrees with the analysis of Schäfer and Wilczek [13]. It does not agree with that of Hong *et al.* [12], because they neglected the contribution of electric gluons. Note that our gap equation (72) differs from that of Son [8] and of Schäfer and Wilczek [13] in that we integrate over momenta q , while they integrate over Euclidean energies q_0 . The energy dependence of our gap function is always given

by the quasiparticle mass shell $\phi(K) = \phi(\epsilon_k, \mathbf{k})$. One advantage of our approach is that the extension to nonzero temperature is immediate.

From Eq. (70), the gluon momenta which dominate the contribution of nearly static, transverse gluons are $p^6 \sim M^4(\epsilon_q \pm \epsilon_k)^2$, or for energies ϵ_q, ϵ_k close to the Fermi surface, $p \sim (m_g^2 \phi)^{1/3}$. While these momenta are small relative to the gluon mass m_g , they are much larger than the condensate ϕ . This is why we can use an HDL propagator in the gap equations, neglecting the effects of the condensate.

The approximations which lead to Eq. (72) are only valid to leading logarithmic accuracy, in that we neglect terms of order 1 relative to $\ln(\mu/m_g) \sim \ln(1/g)$. Possible contributions of order 1, which contribute to b'_0 in Eq. (2), are discussed in Sec. V.

III. SOLVING THE GAP EQUATION

The gap equation (72) is an integral equation for the function $\phi_k \equiv \phi(\epsilon_k, \mathbf{k})$. In general, it can only be solved numerically [13]. In this section, we first discuss the parametric dependence of the solution to Eq. (72) on the QCD coupling constant. To this end, it is instructive to understand which terms in Eq. (71) determine the exponent and the prefactor in Eq. (1). We then derive an approximate analytical solution by converting the integral equation (72) into a differential equation. The solution is discussed in detail at zero and at nonzero temperature.

A. Parametric dependence of the solution on the QCD coupling constant

Let us introduce the variable

$$\bar{g} \equiv \frac{g}{3\sqrt{2}\pi}. \quad (74)$$

At $T=0$, the general structure of the gap equation (71) is

$$\phi_k = \frac{\bar{g}^2}{2} \int_0^{\delta} d(q-\mu) \frac{1}{\epsilon_q} \left[\ln\left(\frac{\mu^2}{|\epsilon_q^2 - \epsilon_k^2|}\right) + 2 \ln\left(\frac{b_0}{b'_0 \bar{g}^5}\right) + c \right] \phi_q. \quad (75)$$

The first term, $\sim \ln(\mu^2/|\epsilon_q^2 - \epsilon_k^2|)$, arises from nearly static, transverse gluons. As compared to Eq. (71) we have factored out a term $\sim \ln(M^2/\mu^2)$. The second term, $\sim \ln[b_0/(b'_0 \bar{g}^5)]$, combines this term with the contribution from electric and nonstatic magnetic gluons. The ratio b_0/b'_0 is a well-defined number and given in Eq. (2). These first two terms comprise the leading logarithmic approximation. The last term, c , represents contributions that go beyond leading logarithmic accuracy, such as terms of order 1 in $\int d(q-\mu)/\epsilon_q$, or of higher order, for instance $\sim \int d(q-\mu)$. We have neglected these terms in our derivation of Eq. (71). In Eq. (2), they were written in terms of the undetermined constant b'_0 . We are therefore permitted to choose $c \equiv 2 \ln b'_0$ in the following.

In order to understand which terms are responsible for the exponent and the prefactor in Eq. (1) let us solve Eq. (75)

assuming that the gap function ϕ_q is constant as a function of momentum. This will give the wrong coefficient in the exponent, but suffices to understand the parametric dependence of Eq. (1) on g . For $k=\mu$, $\phi_q=\phi_k=\phi_0=\text{const}$, the $(q-\mu)$ integral in Eq. (75) can be performed to yield ($\delta \gg \phi_0$)

$$1 \approx \bar{g}^2 \left[\frac{1}{2} \ln^2 \left(\frac{2\delta}{\phi_0} \right) + \ln \left(\frac{b_0\mu}{g^5\delta} \right) \ln \left(\frac{2\delta}{\phi_0} \right) \right]. \quad (76)$$

The first term arises from the leading term $\sim \ln(\mu^2/|\epsilon_q^2 - \epsilon_k^2|)$ in Eq. (75), while the second comes from the leading logarithmic term $\sim \ln[b_0\mu/(b_0'g^5\delta)]$. The quadratic equation (76) for $\ln(2\delta/\phi_0)$ has the solution

$$\ln \left(\frac{2\delta}{\phi_0} \right) \approx -\ln \left(\frac{b_0\mu}{g^5\delta} \right) + \sqrt{\ln^2 \left(\frac{b_0\mu}{g^5\delta} \right) + \frac{2}{\bar{g}^2}}. \quad (77)$$

In weak coupling, the term $\sim 2/\bar{g}^2$ dominates the right-hand side, so that we can expand the square root. This term then gives rise to the exponent in $1/\bar{g}$ for ϕ_0 . The term $\sim \ln[b_0\mu/(g^5\delta)]$ in Eq. (77) gives rise to the prefactor of the exponential. In this way we obtain

$$\phi_0 \approx 2 \frac{b_0}{g^5} \mu \exp \left(-\frac{\sqrt{2}}{g} \right) [1 + O(g)]. \quad (78)$$

Note that, to leading order in g , the dependence on the cutoff δ cancels in the final result. Equation (78) is rather similar to Eq. (1). The difference is that, due to our (erroneous) assumption of a constant gap function, the coefficient in the exponent is incorrect, $\sqrt{2}$, instead of $\pi/2$.

B. Converting the integral equation into a differential equation

The gap equation (72) can be solved analytically by approximating the logarithm under the integral. As in [8], we replace

$$\frac{1}{2} \ln \left(\frac{b^2\mu^2}{|\epsilon_q^2 - \epsilon_k^2|} \right) \rightarrow \ln \left(\frac{b\mu}{\epsilon_q} \right) \theta(q-k) + \ln \left(\frac{b\mu}{\epsilon_k} \right) \theta(k-q), \quad (79)$$

and the gap equation (72) becomes

$$\phi_k \approx \bar{g}^2 \left[\ln \left(\frac{b\mu}{\epsilon_k} \right) \int_0^{k-\mu} \frac{d(q-\mu)}{\epsilon_q} \tanh \left(\frac{\epsilon_q}{2T} \right) \phi_q + \int_{k-\mu}^\delta \frac{d(q-\mu)}{\epsilon_q} \tanh \left(\frac{\epsilon_q}{2T} \right) \ln \left(\frac{b\mu}{\epsilon_q} \right) \phi_q \right]. \quad (80)$$

Upon differentiation with respect to k , we see that the gap function ϕ_k monotonously decreases from its maximum at the Fermi surface $k=\mu$ (we assume $\phi_q \geq 0$ for $0 \leq q-\mu \leq \delta$). Let us introduce the variables

$$y \equiv \ln \left(\frac{2b\mu}{q-\mu+\epsilon_q} \right), \quad (81a)$$

$$x \equiv \ln \left(\frac{2b\mu}{k-\mu+\epsilon_k} \right), \quad (81b)$$

$$x^* \equiv \ln \left(\frac{2b\mu}{\epsilon_\mu} \right) \equiv \ln \left(\frac{2b\mu}{\phi} \right), \quad (81c)$$

where $\phi \equiv \phi_\mu \equiv \phi(\epsilon_\mu, \mu \hat{\mathbf{k}})$ is the value of the gap at the Fermi surface. Obviously, $x^* \geq x, y$. As $\delta \ll m_g \ll \mu \ll b\mu$ [cf. Eq. (73)], both x and y are much larger than 1. In terms of these new variables,

$$\epsilon_q = b\mu e^{-y} \left[1 + \left(\frac{\phi(y)}{\phi} e^{-(x^*-y)} \right)^2 \right] \equiv \epsilon(y), \quad (82a)$$

$$\epsilon_k = b\mu e^{-x} \left[1 + \left(\frac{\phi(x)}{\phi} e^{-(x^*-x)} \right)^2 \right] = \epsilon(x), \quad (82b)$$

where we defined a new function $\epsilon(y)$.

The transformation to the new variable y is natural, because

$$dy = -\frac{d(q-\mu)}{\epsilon_q} \quad (83)$$

is the measure for integration, without any further Jacobian. It is similar to Son's variable $y_{\text{Son}} = \ln(\mu/q_0)$. For Son's variable, however, $dy_{\text{Son}} = -dq_0/q_0$, so that in the gap equation, it is necessary to include a Jacobian for the transformation from q_0 to y_{Son} . This Jacobian does not affect his results for the parametric dependence of the gap function on g , but to leading logarithmic accuracy, it does affect the prefactor and the shape of the gap function; cf. discussion at the end of Sec. III C.

In the new variables x, y the approximate gap equation reads

$$\phi(x) \approx \bar{g}^2 \left[x \int_x^{x^*} dy \tanh \left(\frac{\epsilon(y)}{2T} \right) \phi(y) + \int_{\ln(b\mu/\delta)}^x dy y \tanh \left(\frac{\epsilon(y)}{2T} \right) \phi(y) \right], \quad (84)$$

with $\epsilon(y)$ given by Eq. (82a). Here, we have neglected terms

$$\sim \ln[1 + (\phi(y)/\phi)^2 e^{-2(x^*-y)}] \ll y$$

and

$$\sim \ln[1 + (\phi(x)/\phi)^2 e^{-2(x^*-x)}] \ll x.$$

This is a good approximation, as the value of the logarithms is bounded from above by $\ln 2 \approx 0.693$, while $x, y \geq \ln(b\mu/\delta) \gg 1$. Differentiating with respect to x yields

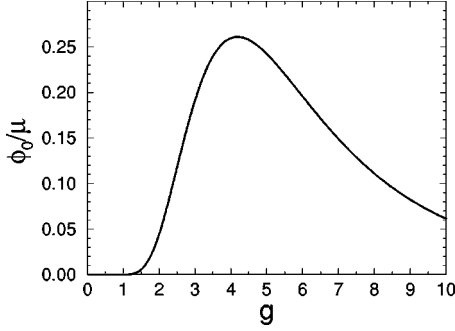


FIG. 1. ϕ_0/μ as function of g . We have set the undetermined constant b'_0 in Eq. (2) equal to 1.

$$\frac{d}{dx} \phi(x) \approx \bar{g}^2 \int_x^{x^*} dy \tanh\left(\frac{\epsilon(y)}{2T}\right) \phi(y), \quad (85a)$$

$$\frac{d^2}{dx^2} \phi(x) \approx -\bar{g}^2 \tanh\left(\frac{\epsilon(x)}{2T}\right) \phi(x). \quad (85b)$$

This is the generalization of Son's equation for the gap function to nonzero temperature.

C. Zero temperature

The approximation (79) has succeeded to convert the original integral equation into the differential equation (85b). For nonzero T , however, because $\epsilon(x)$ is a complicated function of x , this equation still requires a numerical solution. On the other hand, for $T=0$ the solution is simply a trigonometric function. Determining its phase and amplitude from the values of $\phi(x^*)$ and $d\phi/dx$ at x^* , we obtain

$$\phi(x) = \phi_0 \cos[\bar{g}(x^* - x)]. \quad (86)$$

The value of the zero-temperature gap function at the Fermi surface, ϕ_0 , can now be obtained by inserting the solution (86) into the approximate gap equation for $x=x^*$. This yields

$$\phi_0 = 2\delta \exp\left[-\frac{1}{\bar{g}} \arctan\left(\frac{1}{\bar{g} \ln(b\mu/\delta)}\right)\right]. \quad (87)$$

The dependence on the momentum cutoff δ is spurious: in weak coupling, $\bar{g} \ll 1$, we may expand the arctan with the result

$$\phi_0 = 2b\mu \exp\left(-\frac{\pi}{2\bar{g}}\right) \times [1 + O(\bar{g}^2)]. \quad (88)$$

This is identical to Eq. (1), except that here the undetermined constant b'_0 is equal to 1, since we computed only to leading logarithmic accuracy and dropped terms of order 1 in the gap equation.

While our analysis is strictly valid only for small values of g , it is instructive to extrapolate to strong coupling. The behavior of ϕ_0 as function of g is shown in Fig. 1. One observes that ϕ_0 has a maximum at a coupling constant g

≈ 4.2 . The maximum value is quite large, $\phi_0 \approx 0.26\mu$, due to the large prefactor b_0 , Eq. (2), which has important implications for phenomenology [15].

To leading order in \bar{g} , $x^* \equiv \pi/(2\bar{g})$, such that

$$\phi(x) = 2b\mu \exp\left(-\frac{\pi}{2\bar{g}}\right) \sin(\bar{g}x). \quad (89)$$

The gap function peaks at the Fermi surface, $x=x^*$, and varies over a region $x^* - x \sim 1/\bar{g}$. This implies that the gap integral is dominated by momenta exponentially close to the Fermi surface, $\epsilon_q \sim b\mu e^{-y} \ll m_g$. For example, when $q - \mu \sim m_g$, and consequently $y \sim 1$, $\sin(\bar{g}y) \sim \bar{g}y$, and the gap function is \bar{g} times smaller than at the Fermi surface. Physically, this dependence of the gap function on momentum reflects the fact that single-gluon exchange is dominated by forward-angle scattering [15].

The effect of using the variable y , Eq. (81a), instead of a variable $z \equiv \ln(b\mu/\epsilon_q)$ analogous to Son's variable $y_{\text{Son}} \equiv \ln(\mu/q_0)$ [8,13] is the appearance of a prefactor 2 in Eq. (89), as well as a factor of 2 under the logarithm in $x^* = \ln(2b\mu/\phi)$. These factors of 2 were found empirically in a numerical analysis by Schäfer and Wilczek [13].

D. Nonzero temperature

At nonzero temperature, the gap function depends on both x and T . In this subsection we denote this dependence by $\phi(x, T)$. The value of $\phi(x, T)$ at the Fermi surface is denoted by $\phi(T)$. As before, $\phi_0 = \phi(0)$.

In weak coupling, we can compute $\phi(x, T)$ by assuming $\phi(x, T) \approx \phi(T) \phi(x, 0)/\phi_0$. In other words, the x dependence of the gap function is taken to be the same as at zero temperature, so that the only effect of nonzero temperature is to change the overall magnitude of the gap function. We first present this calculation, and then discuss why, in weak coupling, it is reasonable to assume that the gap function as function of x does not change when the temperature is varied. Finally, we verify this assumption by numerical calculations.

For reference, we review how the solution to a BCS-type gap equation changes with temperature. Taking the BCS coupling constant to be G , the gap equation is of the form

$$\phi(T) = G^2 \int_0^\Lambda \frac{d(q-\mu)}{\epsilon_q} \tanh\left(\frac{\epsilon_q}{2T}\right) \phi(T),$$

$$\epsilon_q = \sqrt{(q-\mu)^2 + \phi(T)^2}. \quad (90)$$

In BCS-type theories, the momentum dependence of the gap equation can be ignored, so that we just have a fixed-point equation which determines $\phi(T)$. Besides the trivial solution, $\phi(T) = 0$, at sufficiently small temperatures there is also a nontrivial solution $\phi(T) \neq 0$. It is determined by solving the equation

$$1 = G^2 \int_0^\Lambda \frac{d(q-\mu)}{\epsilon_q} \tanh\left(\frac{\epsilon_q}{2T}\right). \quad (91)$$

At zero temperature, the solution is

$$1 \simeq G^2 \ln\left(\frac{2\Lambda}{\phi_0}\right), \quad \phi_0 \simeq 2\Lambda \exp\left(-\frac{1}{G^2}\right). \quad (92)$$

The gap equation requires us to introduce a cutoff, Λ , but all that matters is that the cutoff be much larger than the value of the gap at zero temperature, $\Lambda \gg \phi_0$.

With increasing T , the thermal factor $\tanh(\epsilon_q/2T)$ reduces the integrand in Eq. (91), so that $\phi(T)$ has to decrease in order to achieve equality of right- and left-hand sides of Eq. (91). Above a critical temperature, T_c , this is no longer possible and we only have the trivial solution, $\phi(T)=0$, $T \geq T_c$.

Let us investigate in more detail how the balance between the left- and right-hand sides of Eq. (91) is achieved at non-zero temperature. We divide the integration region in Eq. (91) into two pieces, for $q-\mu$ smaller or larger than $\kappa\phi_0$, where κ is some pure number, which is assumed to be large. The first region corresponds to momenta near the Fermi surface, $0 \leq q-\mu \leq \kappa\phi_0$. Although $\kappa \gg 1$, because the gap is *exponentially small* in the coupling constant, Eq. (92), in weak coupling this region constitutes only a rather small contribution to the complete gap integral in Eq. (91).

The bulk of the integral comes from the region of momenta away from the Fermi surface, $\kappa\phi_0 \leq q-\mu \leq \Lambda$. The quintessential point of our argument, which we shall apply to the QCD case shortly, is that, for temperatures on the order of ϕ_0 , the thermal factor can be neglected in this region, up to corrections $\sim \exp(-\kappa\phi_0/T)$. The gap equation (91) can therefore be written in the form

$$1 \simeq G^2 \left[\int_0^{\kappa\phi_0} \frac{d(q-\mu)}{\epsilon_q} \tanh\left(\frac{\epsilon_q}{2T}\right) + \int_{\kappa\phi_0}^{\Lambda} \frac{d(q-\mu)}{\epsilon_q} \right]. \quad (93)$$

In the small region very near the Fermi surface, for momenta $0 \leq q-\mu \leq \kappa\phi_0$, the thermal factor must be retained.

In weak coupling, $G \ll 1$, the region away from the Fermi surface almost saturates the 1 on the left-hand side of the gap equation (93). To see this, we compute the contribution of this region to the right-hand side,

$$G^2 \int_{\kappa\phi_0}^{\Lambda} \frac{d(q-\mu)}{\epsilon_q} \simeq G^2 \ln\left(\frac{\Lambda}{\kappa\phi_0}\right) \simeq 1 - G^2 \ln(2\kappa), \quad (94)$$

where we used the solution (92) at $T=0$. Hence, in order to satisfy the gap equation (93), the first integral in Eq. (93) has to balance the term $G^2 \ln(2\kappa)$,

$$G^2 \ln(2\kappa) \simeq G^2 \int_0^{\kappa\phi_0} \frac{d(q-\mu)}{\epsilon_q} \tanh\left(\frac{\epsilon_q}{2T}\right). \quad (95)$$

This equation can be written in a more concise form. Note that

$$\int_0^{\kappa\phi_0} \frac{d(q-\mu)}{\epsilon_q^0} \simeq \ln(2\kappa), \quad (96)$$

where $\epsilon_q^0 = \sqrt{(q-\mu)^2 + \phi_0^2}$ is the quasiparticle excitation energy at zero temperature. We therefore replace the term $\ln(2\kappa)$ in Eq. (95) by this integral,

$$0 \simeq G^2 \int_0^{\kappa\phi_0} d(q-\mu) \left[\frac{1}{\epsilon_q} \tanh\left(\frac{\epsilon_q}{2T}\right) - \frac{1}{\epsilon_q^0} \right]. \quad (97)$$

The same result could have been obtained directly, by subtracting Eq. (91) at zero temperature from Eq. (91) at $T \neq 0$, and using the fact that, for momenta $q-\mu \geq \kappa\phi_0$, $\epsilon_q \simeq \epsilon_q^0$, so that the contributions to the integrals away from the Fermi surface cancel in the subtraction process. The integral in Eq. (97) is finite in the infrared, even for $\phi(T)=0$, since $\tanh(x)/x \rightarrow 1$ as $x \rightarrow 0$.

Dividing all quantities with dimension of energy by ϕ_0 , one realizes that Eq. (97) determines the ratio $\phi(T)/\phi_0$ as a function of T/ϕ_0 . Note that this ratio is independent of the cutoff Λ , as well as the coupling constant G , since G^2 is just an overall constant in Eq. (97) which we can divide out.

Equation (97) has the following interpretation. As mentioned above, the 1 on the left-hand side of the gap equation (93) is almost completely saturated by momenta away from the Fermi surface, $\kappa\phi_0 \leq q-\mu \leq \Lambda$, where thermal corrections are negligible. Thermal effects become important in a small region near the Fermi surface, $0 \leq q-\mu \leq \kappa\phi_0$. It is only in this region that the change of the gap function with temperature has to compensate for the presence of the thermal factor. The ratio $\phi(T)/\phi_0$ is therefore *completely* determined by investigating how the gap equation changes with T in a small region around the Fermi surface.

In Eq. (97), we are allowed to send $\kappa \rightarrow \infty$, as done in Eq. (10) of [15], because $\tanh x \rightarrow 1$ for $x \rightarrow \infty$, and $\epsilon_q \rightarrow \epsilon_q^0$ for $q-\mu \rightarrow \infty$. The ratio $\phi(T)/\phi_0$ is therefore not only independent of the cutoff Λ and the coupling constant G , but also of κ . However, sending $\kappa \rightarrow \infty$ somewhat obscures the fact that only a small region around the Fermi surface controls how $\phi(T)$ changes with temperature.

Equation (97) cannot be evaluated analytically for arbitrary T , although it is easy to solve numerically; as is well known, the transition is of second order, with $\phi(T) \rightarrow 0$ as $T \rightarrow T_c$. At the critical temperature T_c , however, one can evaluate Eq. (97) analytically:

$$\int_0^{\infty} d(q-\mu) \left[\frac{1}{\epsilon_q} \tanh\left(\frac{\epsilon_q}{2T_c}\right) - \frac{1}{\epsilon_q^0} \right] \simeq \ln\left(\frac{\zeta\phi_0}{2T_c}\right) = 0, \quad (98)$$

$$\zeta = \frac{2e^\gamma}{\pi} \simeq 1.13.$$

Here $\gamma \simeq 0.577$ is the Euler-Mascheroni constant. The solution is

$$\frac{T_c}{\phi_0} = \frac{\zeta}{2} = 0.567, \quad (99)$$

which is the usual result in BCS theory [1,2].

We now go through a similar computation for QCD, neglecting the change in the x dependence of the gap function

with temperature, $\phi(x,T) \approx \phi(T) \phi(x,0)/\phi_0$. Consider the gap equation (84) for $x=x^*$, i.e., for the gap function at the Fermi surface, $\phi(T)$. Assuming $T < T_c$, and taking the non-trivial solution $\phi(T) \neq 0$, we can divide both sides by $\phi(T)$. We obtain

$$1 \approx \bar{g}^2 \int_{\ln(b\mu/\delta)}^{x^*} dy y \tanh\left(\frac{\epsilon(y)}{2T}\right) \frac{\phi(y,0)}{\phi_0}. \quad (100)$$

This is the equation analogous to Eq. (91). We now assume that the critical temperature is on the order of the value of the condensate at zero temperature, ϕ_0 . In analogy to the treatment for BCS-like theories, we divide the region of integration into one in which $0 \leq q - \mu \leq \kappa\phi_0$ and one in which $\kappa\phi_0 \leq q - \mu \leq \delta$. As before, for momenta away from the Fermi surface the thermal factor is neglected. Using $\phi(y,0)/\phi_0 = \sin(\bar{g}y)$, we obtain

$$1 \approx \bar{g}^2 \left[\int_{x_\kappa}^{x^*} dy y \tanh\left(\frac{\epsilon(y)}{2T}\right) \sin(\bar{g}y) + \int_{\ln(b\mu/\delta)}^{x_\kappa} dy y \sin(\bar{g}y) \right], \quad (101)$$

which is analogous to Eq. (93). Following the definition of the variable x in Eq. (81b), here we introduced $x_\kappa = \ln[b\mu/(\kappa\phi_0)]$. Again, in weak coupling the 1 on the left-hand side is almost completely saturated by the integration region away from the Fermi surface. To see this, we compute the respective integral in a power series expansion in \bar{g} :

$$\bar{g}^2 \int_{\ln(b\mu/\delta)}^{x_\kappa} dy y \sin(\bar{g}y) \approx 1 - \frac{\pi}{2} \bar{g} \ln(2\kappa) + O(\bar{g}^2). \quad (102)$$

In order to satisfy Eq. (101), the integral over the region very near the Fermi surface has to compensate the terms of order $O(\bar{g})$ in Eq. (102),

$$\bar{g}^2 \int_{x_\kappa}^{x^*} dy y \tanh\left(\frac{\epsilon(y)}{2T}\right) \sin(\bar{g}y) \approx \frac{\pi}{2} \bar{g} \ln(2\kappa) + O(\bar{g}^2). \quad (103)$$

To see how this compensation works, we expand the various terms on the left-hand side in powers of \bar{g} . As $x^* = \pi/(2\bar{g})$ and $x_\kappa = x^* - \ln(2\kappa)$, y is of order x^* in the whole integration region, up to corrections of order \bar{g} . Note that this is equivalent to approximating the factor $\ln(b\mu/\epsilon_q)$ by $\ln(2b\mu/\phi_0)$. For the momentum dependence of the gap function, this has the consequence that $\sin(\bar{g}y) = 1 + O(\bar{g})$; i.e., to leading order in weak coupling, the gap function can be taken to be constant, $\phi(y,0) \approx \phi_0$. In this way one obtains

$$\frac{\pi}{2} \bar{g} \ln(2\kappa) \approx \frac{\pi}{2} \bar{g} \int_0^{\kappa\phi_0} \frac{d(q-\mu)}{\epsilon_q} \tanh\left(\frac{\epsilon_q}{2T}\right) + O(\bar{g}^2), \quad (104)$$

where we reverted the integration variable y into $q - \mu$. With Eq. (96), we can write this as

$$0 \approx \frac{\pi}{2} \bar{g} \int_0^{\kappa\phi_0} d(q-\mu) \left[\frac{1}{\epsilon_q} \tanh\left(\frac{\epsilon_q}{2T}\right) - \frac{1}{\epsilon_q^0} \right] + O(\bar{g}^2). \quad (105)$$

Apart from the prefactor (which can be divided out), to leading order in weak coupling, Eq. (105) is the same as in BCS-type theories, Eq. (97). Thus, also the ratio $\phi(T)/\phi_0$ is *identical* to that in BCS. Given the very different nature of the gap equation, this is a remarkable result.

How can we claim that we can reliably compute $\phi(T)/\phi_0$ to leading order in weak coupling, although we cannot compute the overall magnitude of the condensate at zero temperature, the constant b'_0 in Eq. (2)? To understand this, consider the counting of powers of g in the gap equation; for this, it suffices to use the approximations of Sec. III A.

From Eq. (76) we have seen that the exponential in $1/g$ arises from terms $\sim g^2 \ln^2(2\delta/\phi_0)$. Since $\phi_0 \sim \exp(-1/g)$, these terms are of order 1, and therefore of the same order as the left-hand side of Eq. (76). Analogously, in the nonzero-temperature gap equation (101), terms of order 1 arise from the region of momenta away from the Fermi surface, and thus balance the 1 on the left-hand side. As temperature effects are negligible in this region, we conclude that the exponential behavior $\sim \exp(-1/g)$ of the gap cannot change with temperature.

The prefactor of the exponential is determined by terms $\sim g^2 \ln(2\delta/\phi_0) \sim g$ in the gap equation (76). These include *all* terms of this order, i.e., the leading logarithmic terms as well as terms of order 1, which give rise to b'_0 . From Eq. (103) we realize that temperature effects also enter at order g . These effects therefore change the prefactor of the exponential. In the above discussion, we have determined the change of the gap equation with temperature to leading order in g , or in other words, we have determined the prefactor at nonzero temperature. To leading order in g , the result is that the prefactor changes precisely in the same way as in BCS-like theories.

To understand how the gap function changes with *both* x and T , consider first the region just below the critical temperature. Even though the overall magnitude of the gap, $\phi(T)$, is small, we can still consider $\phi(x,T)/\phi(T)$; even as $T \rightarrow T_c$, this ratio remains of order 1. Then near the Fermi surface, the gap function *must* change due to thermal effects: after all, the variable $x^*(T) = \ln[2b\mu/\phi(T)]$ diverges as $T \rightarrow T_c$, when $\phi(T) \rightarrow 0$.

To understand the change in the gap function, consider energies small relative to the temperature, $\epsilon(x) < T$. In this limit, the thermal factor $\tanh[\epsilon/(2T)] \approx \epsilon/(2T)$. Using the definition of the variable x , Eq. (85b) is approximately

$$\left(\epsilon \frac{d}{d\epsilon} \right)^2 \phi(\epsilon, T) \approx -\bar{g}^2 \left(\frac{\epsilon}{2T} \right) \phi(\epsilon, T). \quad (106)$$

About small ϵ , the solution is given as a power series in $\epsilon/(2T)$:

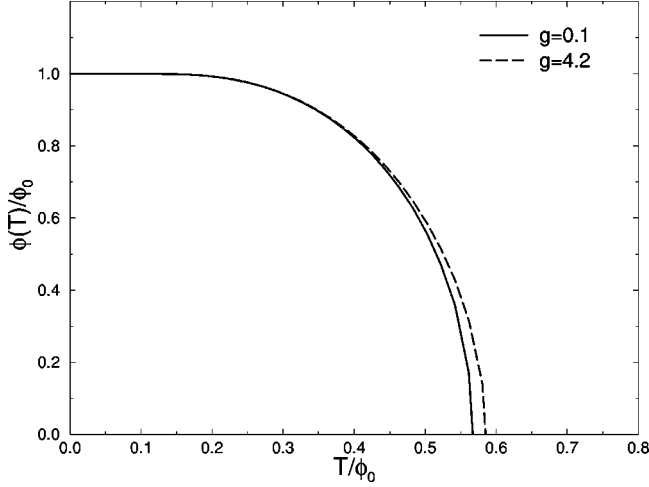


FIG. 2. The gap at the Fermi surface $\phi(T)$, normalized to its zero-temperature value ϕ_0 , as a function of T/ϕ_0 . Solid line, $g=0.1$; dashed line, $g=4.2$.

$$\phi(\epsilon, T) \approx \left[1 - \bar{g}^2 \frac{\epsilon}{2T} + O(\bar{g}^4) \right] \phi(T), \quad T \rightarrow T_c, \quad \epsilon \ll T. \quad (107)$$

Thus when the energy is much less than the temperature, although $x \rightarrow \infty$, the gap function is not $\sim \sin(\bar{g}x)$, as for the zero-temperature gap function, but approaches a constant. That is, due to the thermal factor in the equation for the gap function, the momentum dependence is cut off, and the gap function ‘‘flattens.’’ This is why in our previous calculation we could neglect the momentum dependence of the gap function when the energy is less than $\kappa\phi_0$.

Our analytical results are confirmed by numerical solutions of Eq. (85b) at nonzero temperature. In Fig. 2 we show the gap function at the Fermi surface as a function of temperature. We considered two values of the coupling constant, $g=0.1$ and 4.2 . The first is safely in the weak-coupling regime, while the latter is the value where ϕ_0 has a maximum as a function of g ; cf. Fig. 1. In weak coupling, $\phi(T)/\phi_0$ is indistinguishable from BCS. Surprisingly, even for large $g=4.2$, while T_c is slightly larger than in BCS theory, $T_c/\phi_0 \approx 0.585$, $\phi(T)/\phi_0$ is rather similar to the behavior in BCS-like theories. This is not unlike the situation in strongly coupled BCS, i.e., Eliashberg theory [3], where T_c/ϕ_0 also changes slightly, albeit in the opposite direction.

In Fig. 3(a) we show $\phi(x, T)$ as a function of x at $g=4.2$ for two temperatures, $T=0$ and $T=0.581\phi_0$ which is close to T_c . As the temperature increases, the overall scale of $\phi(x, T)$ decreases, because the condensate is evaporating; cf. Fig. 2. Simultaneously, $x^*(T) = \ln[2b\mu/\phi(T)]$ increases. In Fig. 3(b) we plot $\phi(x, T)/\phi(T)$ as a function of $x/x^*(T)$ at the same two temperatures. As can be seen, once we divide out the overall scale $\phi(T)$, the ratio $\phi(x, T)/\phi(T)$ is relatively insensitive to temperature. At $T=0.581\phi_0$, we observe that the gap function does ‘‘flatten’’ as it approaches the Fermi surface, $x \rightarrow x^*(T)$, as we argued previously on the basis of Eq. (107).

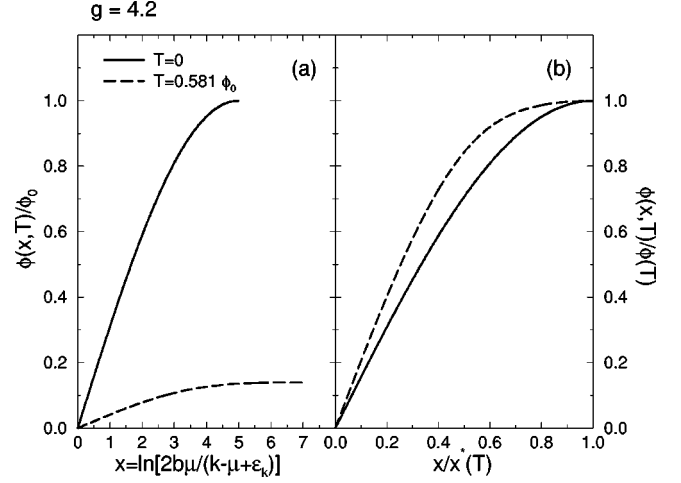


FIG. 3. (a) The gap function $\phi(x, T)$, normalized to the zero-temperature gap function ϕ_0 , as a function of the variable x for $T=0$ (solid line) and $T=0.581\phi_0$ (dashed line), $g=4.2$. (b) The same, but now the gap function is normalized to its value $\phi(T)$ at the Fermi surface at the same temperature, and plotted as function of x normalized to $x^*(T)$. For the sake of simplicity, we have chosen $\delta=b\mu$.

IV. CONDENSATES WITH TOTAL SPIN $J=1$

A. Classification

The gap matrix Φ^+ for a condensate with total spin $J=0$ has the form (19). Generalizing this equation to a condensate with total spin $J=1$ is straightforward. For a $J=1$ condensate, the individual gap functions ϕ_{hs}^e in Eq. (19) are no longer scalar functions in coordinate space, but 3-vectors, ϕ_{hs}^e . These vectors have a component along the direction of \mathbf{k} ,

$$\varphi_{hs}^e(K) \equiv \phi_{hs}^e(K) \cdot \hat{\mathbf{k}}, \quad (108)$$

and two components transverse to this direction,

$$\chi_{hs}^e(K) \equiv \phi_{hs}^e(K) \cdot (1 - \hat{\mathbf{k}}\hat{\mathbf{k}}), \quad (109)$$

such that

$$\phi_{hs}^e(K) \equiv \varphi_{hs}^e(K) \hat{\mathbf{k}} + \chi_{hs}^e(K). \quad (110)$$

The gap matrix Φ^+ is, however, still a scalar in coordinate space. One therefore has to contract the vector indices of χ_{hs}^e with the other independent 3-vector at our disposal, $\boldsymbol{\gamma}$,

$$\chi_{hs}^e(K) \cdot \boldsymbol{\gamma} \equiv \phi_{hs}^e(K) \cdot (1 - \hat{\mathbf{k}}\hat{\mathbf{k}}) \cdot \boldsymbol{\gamma} \equiv \chi_{hs}^e(K) \cdot \boldsymbol{\gamma}_\perp(\mathbf{k}), \quad (111)$$

where we have defined $\boldsymbol{\gamma}_\perp(\mathbf{k}) \equiv (1 - \hat{\mathbf{k}}\hat{\mathbf{k}}) \cdot \boldsymbol{\gamma}$ and used the projector property $(1 - \hat{\mathbf{k}}\hat{\mathbf{k}})^2 \equiv 1 - \hat{\mathbf{k}}\hat{\mathbf{k}}$.

Suppressing color and flavor indices for the moment, the most general ansatz for a gap matrix describing $J=1$ condensates is therefore

$$J=1: \quad \Phi^+(K) = \sum_{h=r,\ell} \sum_{s=\pm} \sum_{e=\pm} [\varphi_{hs}^e(K) + \chi_{hs}^e(K) \cdot \boldsymbol{\gamma}_\perp(\mathbf{k})] \mathcal{P}_{hs}^e(\mathbf{k}). \quad (112)$$

The scalar product $\chi_{hs}^e(K) \cdot \boldsymbol{\gamma}_\perp(\mathbf{k})$ has simple commutation properties with the quasiprojectors $\mathcal{P}_{hs}^e(\mathbf{k})$:

$$\mathcal{P}_h \boldsymbol{\gamma}_\perp(\mathbf{k}) = \boldsymbol{\gamma}_\perp(\mathbf{k}) \mathcal{P}_{-h}, \quad (113a)$$

$$\mathcal{P}_s(\mathbf{k}) \boldsymbol{\gamma}_\perp(\mathbf{k}) = \boldsymbol{\gamma}_\perp(\mathbf{k}) \mathcal{P}_{-s}(\mathbf{k}), \quad (113b)$$

$$\Lambda^e(\mathbf{k}) \boldsymbol{\gamma}_\perp(\mathbf{k}) = \boldsymbol{\gamma}_\perp(\mathbf{k}) [\Lambda^e(\mathbf{k}) - e \alpha_{\mathbf{k}} \boldsymbol{\gamma}_0]. \quad (113c)$$

In the massless limit, $\alpha_{\mathbf{k}}=0$, and $\boldsymbol{\gamma}_\perp$ commutes with the energy projectors.

Instead of contracting the *transverse* components (109) of $\boldsymbol{\phi}_{hs}^e(K)$ with $\boldsymbol{\gamma}$, one could have alternatively also used $\boldsymbol{\phi}_{hs}^e(K)$ itself. The commutation properties for $\boldsymbol{\phi}_{hs}^e \cdot \boldsymbol{\gamma}$, however, are more complicated than for $\chi_{hs}^e \cdot \boldsymbol{\gamma}_\perp(\mathbf{k})$, with additional terms proportional to $\hat{\mathbf{k}}$. The advantage of using $\boldsymbol{\gamma}_\perp(\mathbf{k})$ is that these terms are canceled by the projector $\mathbf{1} - \hat{\mathbf{k}}\hat{\mathbf{k}}$.

Finally, an important question that arises is why we choose $\boldsymbol{\gamma}$ to contract the transverse components of $\boldsymbol{\phi}_{hs}^e$ in Eq. (112). Why not $\boldsymbol{\gamma}_0 \boldsymbol{\gamma}$ or $\boldsymbol{\gamma}_5 \boldsymbol{\gamma}_0 \boldsymbol{\gamma}$? The answer lies again in the commutation properties (113). In the commutation property for $\boldsymbol{\gamma}_0 \boldsymbol{\gamma}_\perp(\mathbf{k})$ or $\boldsymbol{\gamma}_5 \boldsymbol{\gamma}_0 \boldsymbol{\gamma}_\perp(\mathbf{k})$ corresponding to Eq. (113c), the sign of the energy on the right-hand side would be flipped. Physically, this means that such terms represent pairing of particles with antiparticles, and not of particles with particles; cf. discussion of Eq. (119) in Sec. IV C. This is clearly not what happens in a superconductor, where particles form pairs near the Fermi surface.

B. Parity

The $J=1$ condensates can be decomposed according to their transformation properties under parity. Let us first write the interaction term $\bar{\psi}_C \Phi^+ \psi$ in the effective action [9] in the form

$$\begin{aligned} \bar{\psi}_C(K) \Phi^+(K) \psi(K) &= \sum_{h=r,\ell} \sum_{s=\pm} \sum_{e=\pm} \bar{\psi}_C(K) \\ &\times \boldsymbol{\phi}_{hs}^e(K) \cdot [\hat{\mathbf{k}} + \boldsymbol{\gamma}_\perp(\mathbf{k})] \mathcal{P}_{hs}^e(\mathbf{k}) \psi(K). \end{aligned} \quad (114)$$

Let us define new condensate fields

$$\begin{aligned} \boldsymbol{\phi}_\pm^+ &\equiv \frac{1}{2}(\boldsymbol{\phi}_{r+}^+ \pm \boldsymbol{\phi}_{\ell-}^+), \quad \boldsymbol{\phi}_\pm^- \equiv \frac{1}{2}(\boldsymbol{\phi}_{r-}^- \pm \boldsymbol{\phi}_{\ell+}^-), \\ \boldsymbol{\pi}_\pm^+ &\equiv \frac{1}{2}(\boldsymbol{\phi}_{r-}^+ \pm \boldsymbol{\phi}_{\ell+}^+), \quad \boldsymbol{\pi}_\pm^- \equiv \frac{1}{2}(\boldsymbol{\phi}_{r+}^- \pm \boldsymbol{\phi}_{\ell-}^-). \end{aligned} \quad (115)$$

In terms of these fields, the interaction term (114) assumes the form

$$\begin{aligned} \bar{\psi}_C(K) \Phi^+(K) \psi(K) &= \sum_{e=\pm} \bar{\psi}_C(K) \left\{ \boldsymbol{\phi}_+^e(K) \cdot [\hat{\mathbf{k}} + \boldsymbol{\gamma}_\perp(\mathbf{k})] \right. \\ &+ \boldsymbol{\phi}_-^e(K) \cdot [\hat{\mathbf{k}} + \boldsymbol{\gamma}_\perp(\mathbf{k})] \boldsymbol{\gamma}_5 \\ &\times \frac{1+e \boldsymbol{\gamma}_0 \boldsymbol{\gamma} \cdot \hat{\mathbf{k}}}{2} \Lambda^e(\mathbf{k}) \\ &+ \{ \boldsymbol{\pi}_+^e(K) \cdot [\hat{\mathbf{k}} + \boldsymbol{\gamma}_\perp(\mathbf{k})] \\ &+ \boldsymbol{\pi}_-^e(K) \cdot [\hat{\mathbf{k}} + \boldsymbol{\gamma}_\perp(\mathbf{k})] \boldsymbol{\gamma}_5 \} \\ &\left. \times \frac{1-e \boldsymbol{\gamma}_0 \boldsymbol{\gamma} \cdot \hat{\mathbf{k}}}{2} \Lambda^e(\mathbf{k}) \right\} \psi(K). \end{aligned} \quad (116)$$

In the limit $m \rightarrow 0$, $\Lambda^e(\mathbf{k}) \rightarrow (1 + e \boldsymbol{\gamma}_0 \boldsymbol{\gamma} \cdot \hat{\mathbf{k}})/2$, such that the terms proportional to $\boldsymbol{\pi}_\pm^e$ vanish.

Under a parity transformation, $\boldsymbol{\gamma}_0 \rightarrow \boldsymbol{\gamma}_0$, $\boldsymbol{\gamma} \rightarrow -\boldsymbol{\gamma}$, $\boldsymbol{\gamma}_5 \rightarrow -\boldsymbol{\gamma}_5$, and $\mathbf{k} \rightarrow -\mathbf{k}$. Thus, the terms $(1 \pm e \boldsymbol{\gamma}_0 \boldsymbol{\gamma} \cdot \hat{\mathbf{k}})/2$ and the energy projectors do not change under a parity transformation. The parity of $\bar{\psi}_C$ is opposite to that of ψ [9]. A parity transformation leaves the effective action invariant, since the QCD Lagrangian (from which the effective action is derived) does not violate parity explicitly. Thus, if we perform a parity transformation of the interaction term (116), the gap functions $\boldsymbol{\phi}_\pm^e$, $\boldsymbol{\pi}_\pm^e$ must have the same parity as the accompanying Dirac matrices. Consequently, we conclude that $\boldsymbol{\phi}_+^e$, $\boldsymbol{\pi}_+^e$ are parity even, while $\boldsymbol{\phi}_-^e$, $\boldsymbol{\pi}_-^e$ are parity odd.

Two limiting cases are of special interest. If all right-handed, positive-helicity gaps are equal to the left-handed, negative-helicity gaps, $\boldsymbol{\phi}_{r+}^e = \boldsymbol{\phi}_{\ell-}^e$, and all right-handed, negative-helicity gaps are equal to the left-handed, positive-helicity gaps, $\boldsymbol{\phi}_{r-}^e = \boldsymbol{\phi}_{\ell+}^e$, then $\boldsymbol{\phi}_-^e = \boldsymbol{\pi}_-^e = 0$; i.e., the odd-parity gaps vanish, and condensation occurs exclusively in the $J^P = 1^+$ channel. [It is proved in the Appendix that in this case Eq. (116) agrees with the ansatz of Bailin and Love for the $J^P = 1^+$ gaps [4].] On the other hand, if they are equal in magnitude, but different in sign, condensation occurs exclusively in the $J^P = 1^-$ channel.

This is different for the $J=0$ gaps. In that case, one can write down an equation analogous to Eq. (116). The difference is that all vectors $\boldsymbol{\phi}_\pm^e$, $\boldsymbol{\pi}_\pm^e$ are replaced by scalar functions ϕ_\pm^e , π_\pm^e , and the terms $\hat{\mathbf{k}} + \boldsymbol{\gamma}_\perp(\mathbf{k})$ are absent, too. For the parity transformation properties, this has the consequence that if $\phi_{r+}^e = \pm \phi_{\ell-}^e$, $\phi_{r-}^e = \pm \phi_{\ell+}^e$, condensation occurs in the $J^P = 0^\mp$ channel.

C. Ultrarelativistic limit

In the following, we exclusively consider massless fermions. In this case, the helicity projectors (and corresponding indices) become superfluous [cf. Eq. (25)],

$$m=0: \quad \varphi_{hs}^e \rightarrow \varphi_h^e, \quad \chi_{hs}^e \rightarrow \chi_h^e, \quad (117)$$

and the quasiprojectors become true projectors; cf. discussion above [and Eq. (B29) of [9]]. The general ansatz (112) simplifies to

$$J=1, m=0:$$

$$\begin{aligned} \Phi^+(K) &= \sum_{h=r,\ell} \sum_{e=\pm} [\varphi_h^e(K) \\ &+ \chi_h^e(K) \cdot \gamma_\perp(\mathbf{k})] \mathcal{P}_h^e(\mathbf{k}). \end{aligned} \quad (118)$$

In the effective action, the interaction term $\bar{\psi}_C \Phi^+ \psi$ decomposes into four parts on account of the projectors \mathcal{P}_h^e [cf. Eq. (B34) of [9]],

$$\begin{aligned} \bar{\psi}_C(K) \Phi^+(K) \psi(K) &= \sum_{h=r,\ell} \sum_{e=\pm} [\bar{\psi}_{C_h}^e(K) \varphi_h^e(K) \psi_h^e(K) \\ &+ \bar{\psi}_{C-h}^e(K) \chi_h^e(K) \cdot \gamma_\perp(\mathbf{k}) \psi_h^e(K)]. \end{aligned} \quad (119)$$

Here we defined $\psi_h^e \equiv \mathcal{P}_h^e \psi$, and used the commutation properties (113) of γ_\perp . From Eq. (119) it is obvious that the longitudinal gaps correspond to condensation of quarks with the *same* chirality, (*rr*) or (*ℓℓ*). In this respect the longitudinal $J=1$ gaps are similar to the $J=0$ gaps [9]. On the other hand, the transverse $J=1$ gaps correspond to condensation of quarks with *different* chiralities, (*rℓ*) or (*ℓr*).

Equation (119) shows why we do not choose $\gamma_0 \boldsymbol{\gamma}$ or $\gamma_5 \gamma_0 \boldsymbol{\gamma}$ to contract the transverse components of ϕ_{hs}^e in Eq. (112); cf. discussion at the end of Sec. IV A. The extra factors γ_0 or $\gamma_5 \gamma_0$ flip the sign of the energy in Eq. (113c), and the transverse gaps would describe pairing of particles with antiparticles of the same chirality.

D. Color and flavor representations

With the help of the symmetry property [cf. Eq. (B4) of [9]]

$$C \Phi^+(K) C^{-1} = [\Phi^+(-K)]^T, \quad (120)$$

we derive

$$[\varphi_h^e(-K)]^T = -\varphi_h^e(K), \quad [\chi_h^e(-K)]^T = -\chi_{-h}^e(K). \quad (121)$$

The symmetry properties (121) allow us to classify the possible color and flavor representations of the $J=1$ condensates for massless fermions. We assume there are N_f flavors of massless fermions with a global flavor symmetry $SU(N_f)_r \times SU(N_f)_\ell$ and, of course, a local color symmetry $SU(3)_c$. From group theory,

$$2 \times 2 = \mathbf{1}_a + \mathbf{3}_s, \quad 3 \times 3 = \bar{\mathbf{3}}_a + \mathbf{6}_s, \quad (122)$$

where the subscripts *a* and *s* denote antisymmetric or symmetric representations, respectively. For single-gluon exchange, the color-antitriplet channel $\bar{\mathbf{3}}_a^c$ is attractive, and the color-sextet channel $\mathbf{6}_s^c$ is repulsive.

We first discuss the longitudinal condensates φ_h^e . From Eq. (119), the longitudinal $J=1$ condensates only couple quarks of the same chirality, and so do not break the

$SU(N_f)_r \times SU(N_f)_\ell$ flavor symmetry. By Eq. (121), the longitudinal condensates must correspond to a color-flavor representation which is overall antisymmetric.

For $N_f=1$, the flavor representation is trivial, and condensation must occur in the $\bar{\mathbf{3}}_a^c$ channel. This is most likely the favored channel for condensation of quarks of the same flavor, since the $J=0$ gaps are overall symmetric [7,9], and consequently must be in the repulsive $\mathbf{6}_s^c$ channel.

For $N_f=2$, the allowed color-flavor representations are either $(\bar{\mathbf{3}}_a^c, \mathbf{3}_s^f)$, which is favored, or $(\mathbf{6}_s^c, \mathbf{1}_a^f)$. This is in contrast to the $J=0$ gaps, which come in $(\bar{\mathbf{3}}_a^c, \mathbf{1}_a^f)$ or $(\mathbf{6}_s^c, \mathbf{3}_s^f)$. Here the flavor representation refers to either $SU(2)_r$ or $SU(2)_\ell$.

For $N_f=3$, there are $(\bar{\mathbf{3}}_a^c, \mathbf{6}_s^f)$ or $(\mathbf{6}_s^c, \bar{\mathbf{3}}_a^f)$. On the other hand, the $J=0$ gaps are $(\bar{\mathbf{3}}_a^c, \bar{\mathbf{3}}_a^f)$ or $(\mathbf{6}_s^c, \mathbf{6}_s^f)$.

If only longitudinal $J=1$ gaps are present, the parity properties are analogous to the $J=0$ gaps. In particular, since condensates of different chiralities do not mix, the magnitude of the longitudinal $J=1$ gaps will be equal, while their relative phase represents the spontaneous breaking of parity [7,14].

The symmetry relation (121) relates transverse $J=1$ condensates of different chirality. Therefore, we cannot draw general conclusions about the possible color-flavor representations of the transverse $J=1$ gaps. *A priori*, both the symmetric as well as the antisymmetric color and flavor representations are allowed.

Two special cases are of interest. If $\chi_{r,\ell}^e \equiv \chi_{\ell,r}^e$, so that condensation is in the $J^P=1^+$ channel, the color-flavor representations of the transverse $J=1$ gaps are identical to those of the longitudinal $J=1$ gaps. On the other hand, if $\chi_{r,\ell}^e \equiv -\chi_{\ell,r}^e$, so that condensation is in the $J^P=1^-$ channel, they are equal to those of the $J=0$ gaps.

When $N_f \geq 2$, the appearance of transverse $J=1$ gaps must necessarily break the $SU(N_f)_r \times SU(N_f)_\ell$ symmetry to a vectorlike $SU(N_f)$ symmetry. This striking feature arises because the transverse gaps are proportional to γ_\perp , and not, say, $\gamma_0 \gamma_\perp$.

E. Gap equation

In general, condensation can occur in channels with arbitrary total spin J . Therefore, the gap matrix $\Phi^+(K)$ will not simply be of the $J=0$ form (19) or the $J=1$ form (112), but it will be a sum of Eqs. (19) and (112), as well as contain contributions from higher spin $J \geq 2$. We do not attempt to solve this problem in full generality. Instead, we consider the simpler case where the gap matrix contains just $J=0$ and $J=1$ contributions. We also take the fermions to be massless. The gap matrix then assumes the form

$$J=0 \quad \text{and} \quad 1, \quad m=0:$$

$$\begin{aligned} \Phi^+(K) &= \sum_{h=r,\ell} \sum_{e=\pm} [\phi_h^e(K) + \varphi_h^e(K) \\ &+ \chi_h^e(K) \cdot \gamma_\perp(\mathbf{k})] \mathcal{P}_h^e(\mathbf{k}), \end{aligned} \quad (123)$$

where ϕ_h^e denote the $J=0$ gaps, and φ_h^e the longitudinal and χ_h^e the transverse components of the $J=1$ gaps.

The quasiparticle propagator can be computed from Eqs. (7), (8), and (9), and the commutation property (113c). Ignoring the color and flavor structure for the moment, one obtains

$$G^+(Q) = \left\{ \sum_{h=r,\ell} \sum_{e=\pm} (q_0^2 - (q - e\mu)^2 + \{[\phi_h^e(Q)]^\dagger + [\varphi_h^e(Q)]^\dagger - [\chi_{-h}^e(Q)]^\dagger \cdot \boldsymbol{\gamma}_\perp(\mathbf{q})\} \{\phi_h^e(Q) + \varphi_h^e(Q) + \chi_h^e(Q) \cdot \boldsymbol{\gamma}_\perp(\mathbf{q})\}) \mathcal{P}_h^e(\mathbf{q}) \right\}^{-1} [G_0^-(Q)]^{-1}. \quad (124)$$

To invert the term in the large curly brackets, we first have to specify the color-flavor structure of the various condensates. In the following, we just consider the most simple case $N_f = 1$. Let us assume that condensation occurs exclusively in the attractive color-antitriplet channel $\bar{\mathfrak{3}}_a^c$; i.e., $\Phi_{ij}^+ \equiv \epsilon_{ijk} \Phi_k^+$ is an antisymmetric $N_c \times N_c$ matrix in color space, $i, j = 1, \dots, N_c$. In this case, the $J=0$ gaps vanish, $\phi_h^e \equiv 0$, on account of Fermi statistics [7,9]. Since the individual gap functions $\varphi_{hij}^e, \chi_{hij}^e$ are also in the $\bar{\mathfrak{3}}_a^c$ representation, we conclude from Eq. (121) that $\chi_r^e \equiv \chi_\ell^e$. In contrast, φ_r^e and φ_ℓ^e remain *a priori* unrelated.

The term in the large curly brackets in Eq. (124) has an off-diagonal contribution in color space. Since its contribution to G_{ij}^+ is quadratic in ϕ_h^e , we shall neglect it in the following, and consider only the diagonal part, $G_{ij}^+ \approx \delta_{ij} G^+$. Even so, the inversion of the term in the large curly brackets is still cumbersome, due to the presence of terms $\sim \boldsymbol{\gamma}_\perp$. To simplify the treatment, we assume that the $J=1$ gaps are *real valued*. With Eq. (121) this leads to

$$[\varphi_h^e(K)]^\dagger = [\varphi_h^e(-K)]^T \equiv -\varphi_h^e(K),$$

$$[\chi_{-h}^e(K)]^\dagger = [\chi_{-h}^e(-K)]^T \equiv -\chi_h^e(K). \quad (125)$$

This has the consequence that all cross terms $\sim \boldsymbol{\gamma}_\perp$ between the gaps φ_h^e and χ_h^e vanish in Eq. (124). The quasiparticle propagator can now be explicitly computed:

$$G^+(Q) \approx \sum_{h=r,\ell} \sum_{e=\pm} \frac{\mathcal{P}_h^e(\mathbf{q})}{q_0^2 - [\epsilon_q^e(\phi_h^e)]^2} [G_0^-(Q)]^{-1}. \quad (126)$$

The quasiparticle energies are

$$\epsilon_q^e(\phi_h^e) \equiv \left[(q - e\mu)^2 + \sum_{l=1}^{N_c} \phi_{hl}^e \cdot \phi_{hl}^e \right]^{1/2}. \quad (127)$$

Inserting Eq. (126) into the gap equation (5), the same steps that led to Eq. (28) now lead to

$$\Phi_i^+(K) \approx \frac{2}{3} g^2 \frac{T}{V} \sum_Q \gamma^\mu \Delta_{\mu\nu}(K-Q)$$

$$\times \sum_{h=r,\ell} \sum_{e=\pm} \frac{\varphi_{hi}^e(Q) - \chi_{hi}^e(Q) \cdot \boldsymbol{\gamma}_\perp(\mathbf{q})}{q_0^2 - [\epsilon_q^e(\phi_h^e)]^2} \mathcal{P}_{-h}^{-e}(\mathbf{q}) \gamma^\nu. \quad (128)$$

The gap equations for different fundamental colors i decouple; therefore we omit the color index in the following. Taking projections we arrive at the following equation for the longitudinal gap functions:

$$\varphi_h^e(K) \approx \frac{2}{3} g^2 \frac{T}{V} \sum_Q \Delta_{\mu\nu}(K-Q)$$

$$\times \left\{ \frac{\varphi_h^e(Q)}{q_0^2 - [\epsilon_q^e(\phi_h^e)]^2} \text{Tr}[\mathcal{P}_h^e(\mathbf{k}) \gamma^\mu \mathcal{P}_{-h}^{-e}(\mathbf{q}) \gamma^\nu] \right.$$

$$\left. + \frac{\varphi_h^{-e}(Q)}{q_0^2 - [\epsilon_q^{-e}(\phi_h^{-e})]^2} \text{Tr}[\mathcal{P}_h^e(\mathbf{k}) \gamma^\mu \mathcal{P}_{-h}^e(\mathbf{q}) \gamma^\nu] \right\}. \quad (129)$$

This equation is rather similar to Eq. (29). The only difference is the appearance of the transverse gaps in the quasiparticle and quasi-antiparticle energies $\epsilon_q^e(\phi_h^e)$; cf. Eq. (127).

For the transverse gaps, we use the fact that $\chi_r^e = \chi_\ell^e$ to arrive at

$$\chi_h^e(K) \approx \frac{2}{3} g^2 \frac{T}{V} \sum_Q \Delta_{\mu\nu}(K-Q) \left\{ \frac{\chi_h^e(Q)}{q_0^2 - [\epsilon_q^e(\phi_h^e)]^2} \right.$$

$$\times \frac{1}{2} \text{Tr}[\boldsymbol{\gamma} \Lambda^{-e}(\mathbf{q}) \gamma^\nu \Lambda^e(\mathbf{k}) \boldsymbol{\gamma}_\perp(\mathbf{k}) \gamma^\mu]$$

$$+ \frac{\chi_h^{-e}(Q)}{q_0^2 - [\epsilon_q^{-e}(\phi_h^{-e})]^2}$$

$$\left. \times \frac{1}{2} \text{Tr}[\boldsymbol{\gamma} \Lambda^e(\mathbf{q}) \gamma^\nu \Lambda^e(\mathbf{k}) \boldsymbol{\gamma}_\perp(\mathbf{k}) \gamma^\mu] \right\}. \quad (130)$$

Taking the Coulomb gauge for the gluon propagator, Eq. (30), and computing the traces similar to Eqs. (31), we obtain

$$\chi_h^e(K) \approx \frac{2}{3} g^2 \frac{T}{V} \sum_Q \left\{ \frac{\chi_h^e(Q)}{q_0^2 - [\epsilon_q^e(\phi_h^e)]^2} \cdot \left(\mathbf{1} \frac{1 + \hat{\mathbf{k}} \cdot \hat{\mathbf{q}}}{2} - \hat{\mathbf{k}} \frac{\hat{\mathbf{k}} + \hat{\mathbf{q}}}{2} \right) \right.$$

$$\times \left[\Delta_l(K-Q) - \Delta_t(K-Q) \left(1 - \frac{(k-q)^2}{(\mathbf{k}-\mathbf{q})^2} \right) \right]$$

$$+ \frac{\chi_h^{-e}(Q)}{q_0^2 - [\epsilon_q^{-e}(\phi_h^{-e})]^2} \cdot \left(\mathbf{1} \frac{1 - \hat{\mathbf{k}} \cdot \hat{\mathbf{q}}}{2} - \hat{\mathbf{k}} \frac{\hat{\mathbf{k}} - \hat{\mathbf{q}}}{2} \right)$$

$$\left. \times \left[\Delta_l(K-Q) - \Delta_t(K-Q) \left(1 - \frac{(k+q)^2}{(\mathbf{k}-\mathbf{q})^2} \right) \right] \right\}. \quad (131)$$

Neglecting the antiparticle contribution, and taking $k=q=\mu$, as well as $\mathbf{k}=\mathbf{q}$ [the collinear limit; in Eq. (70) this corresponds to neglecting terms of order p^2], we obtain, for the transverse quasiparticle gap,

$$\chi_h^+(K) \approx \frac{2}{3} g^2 \frac{T}{V} \sum_Q \frac{\chi_h^+(Q)}{q_0^2 - [\epsilon_q^+(\phi_h^+)]^2} \times [\Delta_l(K-Q) - \Delta_l(K-Q)]. \quad (132)$$

To leading logarithmic order, the gap equation for the transverse gap is *identical* to that for the longitudinal gap. To see this directly, one computes the traces in Eq. (129). One obtains an equation very similar to Eq. (32). Now one computes the angular factors for $\mathbf{k}=\mathbf{q}$, $k=q=\mu$:

$$\frac{1 + \hat{\mathbf{k}} \cdot \hat{\mathbf{q}}}{2} \approx 1, \quad -\frac{3 - \hat{\mathbf{k}} \cdot \hat{\mathbf{q}}}{2} + \frac{1 + \hat{\mathbf{k}} \cdot \hat{\mathbf{q}}}{2} \frac{(k-q)^2}{(\mathbf{k}-\mathbf{q})^2} \approx -1, \quad (133)$$

which proves our assertion.

Consequently, to this order all $J=1$ gaps are of equal magnitude. Further, the sum of the squares of the $J=1$ gaps satisfies the same gap equation as the square of the $J=0$ gap. This conclusion agrees with Son's renormalization-group analysis [8], who argued that the parametric dependence on g of any spin J gap is the same. We find that even the prefactor is the same to leading logarithmic accuracy. Our results differ from those of Hsu and Schwetz [18], who argued that $J=0$ gaps are favored over those for higher spin.

Beyond leading logarithmic order we suggest that, if $J=0$ gaps are allowed by color-flavor symmetry, they are probably favored over the $J=1$ gaps. If only a $J=1$ gap is allowed, as for $N_f=1$, we believe that either the longitudinal gaps or the transverse gaps with a definite color-flavor representation will be favored. Which one is favored will be determined by the constants b'_0 and b'_1 in Eqs. (2) and (3).

V. CONCLUSIONS

We conclude by addressing effects which can contribute to the constants b'_0 and b'_1 in the condensate, Eqs. (2) and (3). We suggest that our lengthy calculations which led to the result (2) for b_0 may be done much more efficiently by constructing an effective theory for quarks near the Fermi surface, as initiated by Hong [10]. This is presumably the easiest way to calculate b'_0 and b'_1 as well. Nevertheless, we can estimate what kind of effects could contribute to these as of yet undetermined constants. These include the following:

(i) *Gauge dependence of the condensate.* If calculated properly, any physical quantity must be independent of the choice of gauge. For color superconductivity, what is physical is the gap on the quasiparticle mass shell. At nonzero temperature and zero quark density, general arguments due to Kobes, Kunstatter, and Rebhan [27] indicate that the mass shells for quarks and gluons are gauge invariant. Their proof does not extend obviously to nonzero density, but we shall assume that to be the case.

At higher orders, the quasiparticle self-energy, Σ^+ , con-

tains not only the interaction with the condensate, Eq. (8), but also wave-function renormalization. Any apparent gauge dependence in the former must be canceled by the gauge dependence of wave-function renormalization, leaving the quasiparticle mass shell gauge invariant.

It is easy to see that such subtleties do not enter at the order to which we have computed. The gluon propagator in Coulomb gauge, with gauge fixing parameter ξ_C , is given in Eq. (30). Alternatively, one could have taken covariant gauge; with gauge fixing parameter ξ , the covariant gauge propagator was given in Eq. (37) of [23]. We have seen, however, that to the accuracy to which we compute, only the gluon propagator in the static limit, $p_0 \rightarrow 0$, matters. In the static limit, the gauge dependent terms are identical for either the Coulomb or covariant gauge, and appear only as spatially longitudinal terms, $\sim \xi \hat{p}^i \hat{p}^j / p^2$. Consider, for example, how the gauge dependent part of the gluon propagator affects the quasiparticle contribution, $\sim \phi_h^+ / \{q_0^2 - [\epsilon_q^+(\phi_h^+)]^2\}$, to the gap equation for ϕ_h^+ . From the gap equation (29), and using Eqs. (31), this becomes

$$\xi_C \text{Tr}[\mathcal{P}_h^+(\mathbf{k}) \boldsymbol{\gamma} \cdot \hat{\mathbf{p}} \mathcal{P}_h^-(\mathbf{q}) \boldsymbol{\gamma} \cdot \hat{\mathbf{p}}] \sim -\xi_C \frac{1 + \hat{\mathbf{k}} \cdot \hat{\mathbf{q}}}{2} \frac{(k-q)^2}{p^2} \rightarrow 0, \quad k, q \rightarrow \mu. \quad (134)$$

That is, there are gauge dependent terms, but they only contribute to the antiparticle gaps, ϕ_h^- . (Further, the antiparticle gaps must be computed on their proper mass shell. At the Fermi surface, $\epsilon_k^- \sim 2\mu$ is not small, in contrast to $\epsilon_k^+ \sim \phi_0 \ll \mu$.) Consequently, gauge dependent terms in the particle gaps do not appear to even affect the prefactor in the condensate, the constant b'_0 . These conclusions about gauge invariance agree with the results of Schäfer and Wilczek [13]. In contrast, Hong *et al.* [12] argue that the Landau gauge is preferred, as in other approximate treatments of Schwinger-Dyson equations. We insist that in the present example, direct calculation demonstrates gauge invariance without further ado.

(ii) *Wave-function and vertex renormalization.* As noted by Son [8], one can have infrared singular factors for wave-function renormalization. For nonrelativistic fermions, this was noted long ago by Holstein, Norton, and Pincus [28]. (This wave-function renormalization is not the HDL correction discussed by Schäfer and Wilczek [13]; such corrections involve two hard lines, and are down by g^2 .) The dominant corrections involve a very soft transverse gluon on a quark line; this produces gauge-invariant terms of the form $Z-1 \sim g^2 \ln(\mu/\epsilon_q) \sim g$ when $\epsilon_q \sim \phi_0$. This correction was computed by Brown, Liu, and Ren [17], who find that it is a large effect. Besides such wave-function renormalization, one might expect that the Slavnov-Taylor identities would also generate similar corrections for the gluon and for the quark-quark-gluon vertex. This was not found, however, by the authors of [17].

(iii) *Effects of the condensate.* We have computed the gap using an HDL-resummed gluon propagator. This is possible because the momenta which generate the gap are much

larger than the scale of the gap. To see this, note that in the transverse gluon propagator, Eq. (38), Landau damping contributes to the gluon propagator when the momentum $p^6 \sim (m_g^2 \omega)^2$; since the frequency $\omega \sim \phi$, the dominant momenta are $p \sim m_g^{2/3} \phi^{1/3}$, which for small ϕ is much larger than ϕ .

Effects of the condensate on the gluon propagator can be estimated by power counting at large momentum, $p \gg \phi_0$. One would naturally expect that they are $\sim g^2 \phi^2$, but due to an infrared divergence, they are larger, $\sim m_g^2 \phi/p$ [20]. These terms are important when $m_g^2 \phi/p \sim p^2$, or $p \sim m_g^{2/3} \phi^{1/3}$. This is exactly the same scale at which Landau damping operates. These effects will not alter the coefficient of the logarithmic divergence (and hence the exponent), but they will produce terms of order one in the gap equation, which contribute to b'_0 and b'_1 .

(iv) *Damping of the condensate.* In the above, we neglected the fact that the gap function has an imaginary part. To understand this imaginary part, consider first the self-energy for a quark in a Fermi sea. As computed by Le Bellac and Manuel, and by Vanderheyden and Ollitrault [26], away from the edge of the Fermi sea, the quark can decay into another quark and a very soft gluon. This is only possible with a HDL-resummed gluon, whose spectral representation has support from Landau damping in the space-like region. The damping rate of the quark behaves as $\sim g^2 |p - \mu|$, vanishing at the Fermi surface.

From a similar physical process, the gap function acquires a nonzero imaginary part when its momentum is away from the Fermi surface. A quark can scatter into a quark with a different momentum through a very soft gluon. We can estimate the resulting imaginary part of the gap function as follows [15]. If we had not restricted our analysis to the principal value part of the energy denominators arising in Eq. (42), instead of $\ln|\epsilon_q^2 - \epsilon_k^2|$ in Eq. (72) we would have obtained $\ln(\epsilon_q^2 - \epsilon_k^2)$. This logarithm has a cut for $\epsilon_q < \epsilon_k$, giving rise to an imaginary part for ϕ_k ,

$$\text{Im } \phi_k \sim g^{-2} \int_{\phi_0}^{\epsilon_k} \frac{\epsilon_k d\epsilon_q}{\epsilon_q} \phi_q \simeq g^{-2} \ln\left(\frac{\epsilon_k}{\phi_0}\right) \phi_0. \quad (135)$$

Taking $\epsilon_k \sim b\mu e^{-x}$ [cf. Eq. (81b)], momenta exponentially close to the Fermi surface occur when $x \sim x^* = \pi/(2\bar{g})$ (in weak coupling). In this region, the imaginary part of the gap function, $\text{Im } \phi_k \sim \bar{g}^2 (x^* - x) \phi_0$, is *down* by \bar{g} relative to the real part, $\text{Re } \phi_k \sim \sin(\bar{g}x) \phi_0$. At the Fermi surface itself, $x = x^*$, the imaginary part vanishes. Away from the Fermi surface, $\epsilon_k \sim \mu$, so $x \sim 1$, and ϕ_k is strongly damped, with the real and imaginary parts of comparable magnitude, $\text{Re } \phi_k \sim \text{Im } \phi_k \sim \bar{g} \phi_0$.

A gap function with a nonzero imaginary part is actually well known from strongly coupled superconductors, as studied in Eliashberg theory [3]. Damping occurs for a similar reason as here, due to a nonzero imaginary part for the plasmon.

There is no problem in principle with including the damping in the gap function. A spectral representation for the gap

function is introduced, analogous to that of the quark and gluon propagators. The resulting gap integrals are more involved (especially at nonzero temperature), but can be treated in the manner which we employed above.

(v) *Magnetic mass.* As argued in Sec. I, at zero temperature the scale for the magnetic mass is $\sim \mu \exp(-1/g^2)$. It is therefore negligible compared to the scale of the condensate. At nonzero temperature, the scale is no larger than $g^2 T$. For $T \sim \phi_0$, this is down by g^2 , and will only affect the prefactor of the gap to higher order in g .

We conclude by stressing that the determination of the prefactor is not merely an interesting problem in its own right, but because it truly determines the physics of color superconductivity (at least in weak coupling). To the order at which we compute, there is absolutely *no* preference for the condensate to favor spin-0 over spin-1 (or spin-2, etc.). Surely the spin-1 condensate is less favored than spin 0; the ratio of the two condensates is, in weak coupling, a pure number which can be uniquely computed, once one knows how to compute the prefactor in the condensate.

Indeed, perhaps one should entertain a more speculative hypothesis. Even if a $J=0$ gap is favored, maybe there is always some small admixture of higher-spin gaps, and rotational invariance is inevitably broken in the true ground state of color superconductivity.

ACKNOWLEDGMENTS

We acknowledge discussions with D. Blaschke, W. Brown, V. J. Emery, D. K. Hong, S. D. H. Hsu, M. Laine, J. T. Liu, V. N. Muthukumar, K. Rajagopal, H. C. Ren, T. Schäfer, and D. T. Son. We especially thank T. Schäfer and D.T. Son for discussions on the ratio T_c/ϕ_0 . R.D.P. was supported in part by DOE grant DE-AC02-98CH10886. D.H.R. thanks RIKEN, BNL and the U.S. Department of Energy for providing the facilities essential for the completion of this work, and Columbia University's Nuclear Theory Group for continuing access to their computing facilities.

APPENDIX: THE $J^P=1^+$ GAPS

According to the results of Sec. IV B, if condensation occurs exclusively in the $J^P=1^+$ channel, the ansatz for the gap matrix reads (we suppress the dependence of the gap functions on K in the following)

$$J^P=1^+: \quad \Phi^+ = \sum_{e=\pm} \left[\phi_+^e \cdot [\hat{\mathbf{k}} + \boldsymbol{\gamma}_\perp(\mathbf{k})] \frac{1+e\gamma_0 \boldsymbol{\gamma} \cdot \hat{\mathbf{k}}}{2} + \boldsymbol{\pi}_+^e \cdot [\hat{\mathbf{k}} + \boldsymbol{\gamma}_\perp(\mathbf{k})] \frac{1-e\gamma_0 \boldsymbol{\gamma} \cdot \hat{\mathbf{k}}}{2} \right] \Lambda^e(\mathbf{k}). \quad (\text{A1})$$

Now use

$$[\hat{\mathbf{k}} + \boldsymbol{\gamma}_\perp(\mathbf{k})] \frac{1 \pm e \gamma_0 \boldsymbol{\gamma} \cdot \hat{\mathbf{k}}}{2} \Lambda^e(\mathbf{k}) = \hat{\mathbf{k}} \frac{1 \mp e \gamma_0}{4} [(1 \pm \beta_{\mathbf{k}^\mp} \alpha_{\mathbf{k}}) - (1 \pm \beta_{\mathbf{k}^\pm} \alpha_{\mathbf{k}}) \boldsymbol{\gamma} \cdot \hat{\mathbf{k}}] + \boldsymbol{\gamma} \frac{1}{4} [(1 \pm \beta_{\mathbf{k}})(1 \pm e \gamma_0 \boldsymbol{\gamma} \cdot \hat{\mathbf{k}}) \mp \alpha_{\mathbf{k}} \boldsymbol{\gamma} \cdot \hat{\mathbf{k}} + e \alpha_{\mathbf{k}} \gamma_0] \quad (\text{A2})$$

to obtain

$$\begin{aligned} \Phi^+ = & \left[\frac{1 + \beta_{\mathbf{k}^-} \alpha_{\mathbf{k}}}{4} (\boldsymbol{\phi}_+^+ + \boldsymbol{\phi}_+^-) + \frac{1 - \beta_{\mathbf{k}^+} \alpha_{\mathbf{k}}}{4} (\boldsymbol{\pi}_+^+ + \boldsymbol{\pi}_+^-) \right] \cdot \hat{\mathbf{k}} + \left[-\frac{1 + \beta_{\mathbf{k}^-} \alpha_{\mathbf{k}}}{4} (\boldsymbol{\phi}_+^+ - \boldsymbol{\phi}_+^-) + \frac{1 - \beta_{\mathbf{k}^+} \alpha_{\mathbf{k}}}{4} (\boldsymbol{\pi}_+^+ - \boldsymbol{\pi}_+^-) \right] \cdot \hat{\mathbf{k}} \gamma_0 \\ & + \left[-\frac{1 + \beta_{\mathbf{k}^+} \alpha_{\mathbf{k}}}{4} (\boldsymbol{\phi}_+^+ + \boldsymbol{\phi}_+^-) - \frac{1 - \beta_{\mathbf{k}^-} \alpha_{\mathbf{k}}}{4} (\boldsymbol{\pi}_+^+ + \boldsymbol{\pi}_+^-) \right] \cdot \hat{\mathbf{k}} \boldsymbol{\gamma} \cdot \hat{\mathbf{k}} + \left[\frac{1 + \beta_{\mathbf{k}^+} \alpha_{\mathbf{k}}}{4} (\boldsymbol{\phi}_+^+ - \boldsymbol{\phi}_+^-) - \frac{1 - \beta_{\mathbf{k}^-} \alpha_{\mathbf{k}}}{4} \right. \\ & \times (\boldsymbol{\pi}_+^+ - \boldsymbol{\pi}_+^-) \left. \right] \cdot \hat{\mathbf{k}} \gamma_0 \boldsymbol{\gamma} \cdot \hat{\mathbf{k}} + \left[\frac{1 + \beta_{\mathbf{k}}}{4} (\boldsymbol{\phi}_+^+ + \boldsymbol{\phi}_+^-) + \frac{1 - \beta_{\mathbf{k}}}{4} (\boldsymbol{\pi}_+^+ + \boldsymbol{\pi}_+^-) \right] \cdot \boldsymbol{\gamma} + \frac{\alpha_{\mathbf{k}}}{4} (\boldsymbol{\phi}_+^+ - \boldsymbol{\phi}_+^- + \boldsymbol{\pi}_+^+ - \boldsymbol{\pi}_+^-) \cdot \boldsymbol{\gamma} \gamma_0 \\ & + \frac{\alpha_{\mathbf{k}}}{4} (-\boldsymbol{\phi}_+^+ - \boldsymbol{\phi}_+^- + \boldsymbol{\pi}_+^+ + \boldsymbol{\pi}_+^-) \cdot \boldsymbol{\gamma} \boldsymbol{\gamma} \cdot \hat{\mathbf{k}} + \left[\frac{1 + \beta_{\mathbf{k}}}{4} (\boldsymbol{\phi}_+^+ - \boldsymbol{\phi}_+^-) - \frac{1 - \beta_{\mathbf{k}}}{4} (\boldsymbol{\pi}_+^+ - \boldsymbol{\pi}_+^-) \right] \cdot \boldsymbol{\gamma} \gamma_0 \boldsymbol{\gamma} \cdot \hat{\mathbf{k}}. \end{aligned} \quad (\text{A3})$$

Bailin and Love's ansatz for a $J^P = 1^+$ gap reads [cf. Eq. (4.24) of [4]; we again suppress the momentum dependence of the gap functions]

$$\begin{aligned} \Delta = & \boldsymbol{\Delta}_1 \cdot \boldsymbol{\gamma} + \boldsymbol{\Delta}_2 \cdot \hat{\mathbf{k}} \boldsymbol{\gamma} \cdot \hat{\mathbf{k}} + i \boldsymbol{\Delta}_3 \times \hat{\mathbf{k}} \cdot \boldsymbol{\gamma} \gamma_5 + \boldsymbol{\Delta}_4 \cdot \hat{\mathbf{k}} + \boldsymbol{\Delta}_5 \cdot \boldsymbol{\gamma} \gamma_0 \\ & + \boldsymbol{\Delta}_6 \cdot \hat{\mathbf{k}} \boldsymbol{\gamma} \cdot \hat{\mathbf{k}} \gamma_0 + \boldsymbol{\Delta}_7 \cdot \hat{\mathbf{k}} \gamma_0 + i \boldsymbol{\Delta}_8 \times \hat{\mathbf{k}} \cdot \boldsymbol{\gamma} \gamma_0 \gamma_5. \end{aligned} \quad (\text{A4})$$

(We added an i in the last term as compared to [4]. This simplifies the notation in the following, but is not essential, as the gap functions are in general complex valued.) With the definition of $\gamma_5 = i \gamma_0 \boldsymbol{\gamma}^1 \boldsymbol{\gamma}^2 \boldsymbol{\gamma}^3$ one computes

$$i \boldsymbol{\Delta} \times \hat{\mathbf{k}} \cdot \boldsymbol{\gamma} \gamma_5 = -\gamma_0 (\boldsymbol{\Delta} \cdot \hat{\mathbf{k}} + \boldsymbol{\Delta} \cdot \boldsymbol{\gamma} \boldsymbol{\gamma} \cdot \hat{\mathbf{k}}) \equiv -\gamma_0 \boldsymbol{\Delta} \cdot \boldsymbol{\gamma}_\perp(\mathbf{k}) \boldsymbol{\gamma} \cdot \hat{\mathbf{k}}, \quad (\text{A5})$$

and rewrites Eq. (A4) as

$$\begin{aligned} \Delta = & (\boldsymbol{\Delta}_4 + \boldsymbol{\Delta}_8) \cdot \hat{\mathbf{k}} + (\boldsymbol{\Delta}_7 - \boldsymbol{\Delta}_3) \cdot \hat{\mathbf{k}} \gamma_0 + \boldsymbol{\Delta}_2 \cdot \hat{\mathbf{k}} \boldsymbol{\gamma} \cdot \hat{\mathbf{k}} - \boldsymbol{\Delta}_6 \cdot \hat{\mathbf{k}} \boldsymbol{\gamma}_0 \boldsymbol{\gamma} \cdot \hat{\mathbf{k}} \\ & + \boldsymbol{\Delta}_1 \cdot \boldsymbol{\gamma} + \boldsymbol{\Delta}_5 \cdot \boldsymbol{\gamma} \gamma_0 + \boldsymbol{\Delta}_8 \cdot \boldsymbol{\gamma} \boldsymbol{\gamma} \cdot \hat{\mathbf{k}} + \boldsymbol{\Delta}_3 \cdot \boldsymbol{\gamma} \gamma_0 \boldsymbol{\gamma} \cdot \hat{\mathbf{k}}. \end{aligned} \quad (\text{A6})$$

Direct comparison of Eqs. (A3) and (A6) reveals

$$\boldsymbol{\Delta}_1 = \boldsymbol{\Delta}_4 = \frac{1 + \beta_{\mathbf{k}}}{4} (\boldsymbol{\phi}_+^+ + \boldsymbol{\phi}_+^-) + \frac{1 - \beta_{\mathbf{k}}}{4} (\boldsymbol{\pi}_+^+ + \boldsymbol{\pi}_+^-), \quad (\text{A7a})$$

$$\boldsymbol{\Delta}_2 = -\boldsymbol{\Delta}_1 + \boldsymbol{\Delta}_8, \quad (\text{A7b})$$

$$\boldsymbol{\Delta}_3 = \frac{1 + \beta_{\mathbf{k}}}{4} (\boldsymbol{\phi}_+^+ - \boldsymbol{\phi}_+^-) - \frac{1 - \beta_{\mathbf{k}}}{4} (\boldsymbol{\pi}_+^+ - \boldsymbol{\pi}_+^-), \quad (\text{A7c})$$

$$\boldsymbol{\Delta}_5 = \boldsymbol{\Delta}_7 = \frac{\alpha_{\mathbf{k}}}{4} (\boldsymbol{\phi}_+^+ - \boldsymbol{\phi}_+^- + \boldsymbol{\pi}_+^+ - \boldsymbol{\pi}_+^-), \quad (\text{A7d})$$

$$\boldsymbol{\Delta}_6 = -\boldsymbol{\Delta}_3 - \boldsymbol{\Delta}_5, \quad (\text{A7e})$$

$$\boldsymbol{\Delta}_8 = \frac{\alpha_{\mathbf{k}}}{4} (-\boldsymbol{\phi}_+^+ - \boldsymbol{\phi}_+^- + \boldsymbol{\pi}_+^+ + \boldsymbol{\pi}_+^-). \quad (\text{A7f})$$

These relations exhibit a redundancy in Bailin and Love's ansatz (A4): only four of the eight 3-vector gap functions $\boldsymbol{\Delta}_1, \dots, \boldsymbol{\Delta}_8$ are independent. The reason for this redundancy is that in Eq. (A4) the transverse components of $\boldsymbol{\Delta}_2, \boldsymbol{\Delta}_4, \boldsymbol{\Delta}_6,$ and $\boldsymbol{\Delta}_7$ never appear, as these gap functions are projected in the longitudinal direction $\hat{\mathbf{k}}$. Furthermore, only the transverse components of $\boldsymbol{\Delta}_3$ and $\boldsymbol{\Delta}_8$ appear on account of Eq. (A5). Finally, the longitudinal components of the remaining two gap functions $\boldsymbol{\Delta}_1$ and $\boldsymbol{\Delta}_5$ can be absorbed by redefining $\boldsymbol{\Delta}_2$ and $\boldsymbol{\Delta}_6$; thus only their transverse components contribute. In this manner, only half of the original 24 gap functions are independent. Physically, this can be understood from the restriction to the positive-parity channel $J^P = 1^+$. Thus, only the four 3-vectors $\boldsymbol{\phi}_+^\pm, \boldsymbol{\pi}_+^\pm$ appear on the right-hand side of Eq. (A7). The other four 3-vectors $\boldsymbol{\phi}_-^\pm, \boldsymbol{\pi}_-^\pm$ do not contribute, as they correspond to pairing in the $J^P = 1^-$ channel.

This said, one can readily derive a more efficient form of Bailin and Love's ansatz (A4), which utilizes both longitudinal and transverse components of the truly independent gap functions. Choosing the latter to be $\boldsymbol{\Delta}_1, \boldsymbol{\Delta}_3, \boldsymbol{\Delta}_5,$ and $\boldsymbol{\Delta}_8,$ we obtain, from Eq. (A4) with Eq. (A7),

$$\begin{aligned} \Delta = & \boldsymbol{\Delta}_1 \cdot [\hat{\mathbf{k}} + \boldsymbol{\gamma}_\perp(\mathbf{k})] + \boldsymbol{\Delta}_3 \cdot [\hat{\mathbf{k}} + \boldsymbol{\gamma}_\perp(\mathbf{k})] \gamma_0 \boldsymbol{\gamma} \cdot \hat{\mathbf{k}} \\ & + \boldsymbol{\Delta}_5 \cdot [\hat{\mathbf{k}} + \boldsymbol{\gamma}_\perp(\mathbf{k})] \gamma_0 + \boldsymbol{\Delta}_8 \cdot [\hat{\mathbf{k}} + \boldsymbol{\gamma}_\perp(\mathbf{k})] \boldsymbol{\gamma} \cdot \hat{\mathbf{k}}. \end{aligned} \quad (\text{A8})$$

It is now also easy to interpret the results obtained by Bailin and Love in [29], where they studied $J^P = 1^+$ condensation in the ultrarelativistic limit. In this limit, $\alpha_{\mathbf{k}} = 0$, thus $\boldsymbol{\Delta}_5 = \boldsymbol{\Delta}_8 = 0$ on account of Eqs. (A7). Bailin and Love discuss two order parameters for condensation in the $J^P = 1^+$ channel, the first being the longitudinal component of $\boldsymbol{\Delta}_4 - \boldsymbol{\Delta}_5 - \boldsymbol{\Delta}_6$, the second being $(\boldsymbol{\Delta}_1 + \boldsymbol{\Delta}_3) \cdot (\boldsymbol{\gamma} - \hat{\mathbf{k}} \boldsymbol{\gamma} \cdot \hat{\mathbf{k}} - i \hat{\mathbf{k}} \times \boldsymbol{\gamma} \gamma_5)$.

From Eqs. (A7), we identify the first with the longitudinal

component of $\Delta_1 + \Delta_3$. From Eq. (A5), we realize that the second is identical to $(\Delta_1 + \Delta_3) \cdot \gamma_{\perp}(\mathbf{k}) (1 - \gamma_0 \boldsymbol{\gamma} \cdot \hat{\mathbf{k}})$; i.e., essentially the transverse components of $\Delta_1 + \Delta_3$. Thus, Bailin and Love discuss two separate gap equations, one for the longitudinal, the other for the transverse components of the

independent gap function $\Delta_1 + \Delta_3$. Although we also find two gap equations for the longitudinal and the transverse gaps (cf. Sec. IV), we do *not* find that they decouple, as the excitation energies (127) contain *both* longitudinal and transverse gap functions.

-
- [1] J. R. Schrieffer, *Theory of Superconductivity* (Benjamin, New York, 1964).
- [2] A. L. Fetter and J. D. Walecka, *Quantum Theory of Many-Particle Systems* (McGraw-Hill, New York, 1971); A. A. Abrikosov, L. P. Gorkov, and I. E. Dzyaloshinski, *Methods of Quantum Field Theory in Statistical Physics* (Dover, New York, 1963).
- [3] D. J. Scalapino, in *Superconductivity*, edited by R. D. Parks (Dekker, New York, 1969), p. 449ff.
- [4] D. Bailin and A. Love, Phys. Rep. **107**, 325 (1984).
- [5] M. Alford, K. Rajagopal, and F. Wilczek, Phys. Lett. B **422**, 247 (1998); R. Rapp, T. Schäfer, E. V. Shuryak, and M. Velkovsky, Phys. Rev. Lett. **81**, 53 (1998); hep-ph/9904353; N. Evans, S. D. H. Hsu, and M. Schwetz, Nucl. Phys. **B551**, 275 (1999); Phys. Lett. B **449**, 281 (1999); J. Berges and K. Rajagopal, Nucl. Phys. **B538**, 215 (1999); T. Schäfer and F. Wilczek, Phys. Lett. B **450**, 325 (1999); G. W. Carter and D. Diakonov, Phys. Rev. D **60**, 016004 (1999); K. Langfeld and M. Rho, hep-ph/9811227; M. Alford, J. Berges, and K. Rajagopal, Nucl. Phys. **B558**, 219 (1999); E. Shuster and D. T. Son, hep-ph/9905448; D. K. Hong, M. Rho, and I. Zahed, Phys. Lett. B **468**, 261 (1999); V. A. Miransky, I. A. Shovkovy, and L. C. R. Wijewardhana, *ibid.* **468**, 270 (1999); R. Casalbuoni and R. Gatto, *ibid.* **464**, 111 (1999); hep-ph/9909419; B. Y. Park, M. Rho, A. Wirzbad, and I. Zahed, hep-ph/991034.
- [6] M. Alford, K. Rajagopal, and F. Wilczek, Nucl. Phys. **B537**, 443 (1999).
- [7] R. D. Pisarski and D. H. Rischke, Phys. Rev. Lett. **83**, 37 (1999).
- [8] D. T. Son, Phys. Rev. D **59**, 094019 (1999).
- [9] R. D. Pisarski and D. H. Rischke, Phys. Rev. D **60**, 094013 (1999).
- [10] D. K. Hong, hep-ph/9812510; hep-ph/9905523.
- [11] T. Schäfer and F. Wilczek, Phys. Rev. Lett. **82**, 3956 (1999); Phys. Rev. D **60**, 074014 (1999).
- [12] D. K. Hong, V. A. Miransky, I. A. Shovkovy, and L. C. R. Wijewardhana, Phys. Rev. D **61**, 056001 (2000).
- [13] T. Schäfer and F. Wilczek, Phys. Rev. D **60**, 114033 (1999).
- [14] R. D. Pisarski and D. H. Rischke, nucl-th/9906050.
- [15] R. D. Pisarski and D. H. Rischke, Phys. Rev. D **61**, 051501 (2000).
- [16] R. D. Pisarski and D. H. Rischke, nucl-th/9907094.
- [17] W. E. Brown, J. T. Liu, and H.-C. Ren, Phys. Rev. D (to be published), hep-ph/9908248.
- [18] S. D. H. Hsu and M. Schwetz, hep-ph/9908310.
- [19] T. Schäfer, hep-ph/9909574; I. A. Shovkovy and L. C. R. Wijewardhana, Phys. Lett. B **470**, 189 (1999).
- [20] N. Evans, J. Hormuzdiar, S. D. H. Hsu, and M. Schwetz, hep-ph/9910313.
- [21] J. O. Andersen, E. Braaten, and M. Strickland, Phys. Rev. Lett. **83**, 2139 (1999); Phys. Rev. D **61**, 014017 (2000); J.-P. Blaizot, E. Iancu, and A. Rebhan, Phys. Rev. Lett. **83**, 2906 (1999).
- [22] B. Freedman and L. D. McLerran, Phys. Rev. D **16**, 1130 (1977); **16**, 1147 (1977); **16**, 1169 (1977); **17**, 1109 (1978); R. Baier and K. Redlich, Phys. Rev. Lett. **84**, 2100 (2000).
- [23] R. D. Pisarski, Physica A **158**, 146 (1989).
- [24] M. Le Bellac, *Thermal Field Theory* (Cambridge University Press, Cambridge, England, 1996).
- [25] J.-P. Blaizot and J.-Y. Ollitrault, Phys. Rev. D **48**, 1390 (1993); H. Vija and M. H. Thoma, Phys. Lett. B **342**, 212 (1995); C. Manuel, Phys. Rev. D **53**, 5866 (1996).
- [26] M. Le Bellac and C. Manuel, Phys. Rev. D **55**, 3215 (1997); B. Vanderheyden and J.-Y. Ollitrault, *ibid.* **56**, 5108 (1997).
- [27] R. Kobes, G. Kunstatter, and A. Rebhan, Phys. Rev. Lett. **64**, 2992 (1990); Nucl. Phys. **B355**, 1 (1991).
- [28] T. Holstein, R. E. Norton, and P. Pincus, Phys. Rev. B **6**, 2649 (1973).
- [29] D. Bailin and A. Love, Nucl. Phys. **B190**, [FS3], 175 (1981).